Aus der
Klinik und Poliklinik für Nuklearmedizin
Klinikum der Ludwig-Maximilians-Universität München
Direktor: Prof. Dr. Rudolf Alexander Werner

Evaluation of synaptic density, neuroinflammation, and β-amyloid in two amyloidosis mouse models

Dissertation
zum Erwerb des Doktorgrades der Naturwissenschaften
an der Medizinischen Fakultät der
Ludwig-Maximilians-Universität München

vorgelegt von
Lea Helena Kunze

aus
Eutin

Jahr
2025

Mit Genehmigung der Medizinischen Fakultät
der Ludwig-Maximilians-Universität München

Betreuerin:	Prof. Dr. Sibylle Ziegler
Zweitgutachter:	Prof. Dr. Dominik Paquet
Dekan:	Prof. Dr. med. Thomas Gudermann
Tag der mündlichen Prüfung:	09. Februar 2026

Übereinstimmungserklärung

LMU LUDWIG-MAXIMILIANS-UNIVERSITÄT MÜNCHEN

Dekanat Medizinische Fakultät
Promotionsbüro

Erklärung zur Übereinstimmung der gebundenen Ausgabe der Dissertation mit der elektronischen Fassung

Kunze, Lea Helena

Name, Vorname

Hiermit erkläre ich, dass die elektronische Version der eingereichten Dissertation mit dem Titel:

Evaluation of synaptic density, neuroinflammation, and β-amyloid in two amyloidosis mouse models

……

in Inhalt und Formatierung mit den gedruckten und gebundenen Exemplaren übereinstimmt.

München, 23.04.2025

Ort, Datum

Lea Helena Kunze

Unterschrift Doktorandin bzw. Doktorand

Affidavit

LMU LUDWIG-MAXIMILIANS-UNIVERSITÄT MÜNCHEN

Dekanat Medizinische Fakultät
Promotionsbüro

Eidesstattliche Versicherung

Kunze, Lea Helena

Name, Vorname

Ich erkläre hiermit an Eides statt, dass ich die vorliegende Dissertation mit dem Titel:

Evaluation of synaptic density, neuroinflammation, and β-amyloid in two amyloidosis mouse models

……

selbständig verfasst, mich außer der angegebenen keiner weiteren Hilfsmittel bedient und alle Erkenntnisse, die aus dem Schrifttum ganz oder annähernd übernommen sind, als solche kenntlich gemacht und nach ihrer Herkunft unter Bezeichnung der Fundstelle einzeln nachgewiesen habe.

Ich erkläre des Weiteren, dass die hier vorgelegte Dissertation nicht in gleicher oder in ähnlicher Form bei einer anderen Stelle zur Erlangung eines akademischen Grades eingereicht wurde.

München, 23.04.2025 — Ort, Datum

Lea Helena Kunze — Unterschrift Doktorandin bzw. Doktorand

Content

Abbreviations

[^{11}C]-UCB-J ... (4R)-1-{[3-(^{11}C)Methylpyridin-4-yl]methyl}-4-(3,4,5-trifluorophenyl)pyrrolidin-2-one
[^{18}F]FBB ... [^{18}F]florbetaben
[^{18}F]F-DED ... [^{18}F]fluorodeprenyl-D2
[^{18}F]FDG ... 2-[^{18}F]deoxy-2-fluoro-D-glucose or [^{18}F]fluordeoxyglucose
[^{18}F]GE-180 ... [^{18}F]flutriciclamide
[^{18}F]UCB-H ... [^{18}F]fluoropyridyl(4-methoxyphenyl)iodonium
AD ... Alzheimer's disease
AICD ... Amyloid intracellular domain
APOE4 ... apolipoprotein E ε4
APP ... amyloid precursor protein
APP^{SAA} ... *App* knock-in mouse model
Aβ ... amyloid-β
Bq ... Becquerel
C99 ... C-terminal fragment 99
CSF ... cerebrospinal fluid
CT ... computer tomography
DNA ... deoxyribonucleic acid
ECL ... electrochemiluminescence
ELISA ... enzyme-linked immunosorbent assay
FACS ... fluorescent-activated cell sorting
FBP ... filtered backprojection
GFAP ... glial fibrillary acidic protein
GLT-1 ... glutamate transporter 1
IDIF ... image derived input function
LC ... liquid chromatography
LOR ... line of response
MAO-B ... monoamine oxidase B
MCI ... mild cognitive impairment
MMSE ... Mini-Mental State Examination
MR ... magnetic resonance
MS ... mass spectrometry
NfL ... neurofilament light chain
PCR ... polymerase chain reaction
PET ... positron emission tomography
PFA ... paraformaldehyde
PSEN1 ... presenilin 1
PSEN2 ... presenilin 2
RNA ... ribonucleic acid

RNASeq .....RNA Sequencing
RT-qPCR.....quantitative reverse transcription-polymerase chain reaction
sAβPP .....soluble amyloid-β precursor protein
SDS-PAGE.....sodium dodecyl sulfate polyacrylamide-gel electrophoresis
SiMoA.....single-molecule array
SPM..... statistical parametric mapping
SUV .....standardized uptake value
SUVr.....standardized uptake value ratio
SV2A ..... synaptic vesicle protein 2A
TSPO..... translocator protein
VLDL.....very low density lipoprotein
VOI .....volume of interest
V_T..... volume of distribution

List of Illustrations

List of Publications

This cumulative dissertation is in accordance with the graduation regulation for natural sciences at the medical faculty of the University of Munich (Ludwig-Maximilians-Universität München) and is based on the following two publications:

First publication:

Kunze, L. H., Palumbo, G., Gnörich, J., Wind-Mark, K., Schaefer, R., Lindner, S., Gildehaus, F.-J., Ziegler, S., & Brendel, M. (2025). Fibrillar amyloidosis and synaptic vesicle protein expression progress jointly in the cortex of a mouse model with β-amyloid pathology. *NeuroImage*, *310*, 121165. https://doi.org/10.1016/j.neuroimage.2025.121165 (**IF: 4.7**)

Second publication:

Xia, D., Lianoglou, S., Sandmann, T., Calvert, M., Suh, J. H., Thomsen, E., Dugas, J., Pizzo, M. E., DeVos, S. L., Earr, T. K., Lin, C.-C., Davis, S., Ha, C., Leung, A. W.-S., Nguyen, H., Chau, R., Yulyaningsih, E., Lopez, I., Solanoy, H., … , **Kunze, L. H.**, … , Sanchez, P. E. (2022). Novel *App* knock-in mouse model shows key features of amyloid pathology and reveals profound metabolic dysregulation of microglia. *Molecular Neurodegeneration*, *17*, 41. https://doi.org/10.1186/s13024-022-00547-7 (**IF: 16.8**)

Further publications

Contributions to the following publications were made:

1. Bartos, L. M., Quach, S., Zenatti, V., Kirchleitner, S. V., Blobner, J., Wind-Mark, K., Kolabas, Z. I., Ulukaya, S., Holzgreve, A., Ruf, V. C., **Kunze, L. H.**, Kunte, S. T., Hoermann, L., Härtel, M., Park, H. E., Groß, M., Franzmeier, N., Zatcepin, A., Zounek, A., … Brendel, M. (2024). Remote Neuroinflammation in Newly Diagnosed Glioblastoma Correlates with Unfavorable Clinical Outcome. *Clinical Cancer Research*, *30*(20), 4618–4634. https://doi.org/10.1158/1078-0432.CCR-24-1563 (**IF: 10.0**)
2. Shojaei, M., Schaefer, R., Schlepckow, K., **Kunze, L. H.**, Struebing, F. L., Brunner, B., Willem, M., Bartos, L. M., Feiten, A., Palumbo, G., Arzberger, T., Bartenstein, P., Parico, G. C., Xia, D., Monroe, K. M., Haass, C., Brendel, M., & Lindner, S. (2024). PET imaging of microglia in Alzheimer's disease using copper-64 labeled TREM2 antibodies. *Theranostics*, *14*(16), 6319–6336. https://doi.org/10.7150/thno.97149 (**IF: 12.4**)
3. Slemann, L., Gnörich, J., Hummel, S., Bartos, L. M., Klaus, C., Kling, A., Kusche-Palenga, J., Kunte, S. T., **Kunze, L. H.**, Englert, A. L., Li, Y., Vogler, L., Katzdobler, S., Palleis, C., Bernhardt, A., Jäck, A., Zwergal, A., Hopfner, F., Roemer-Cassiano, S. N., … Brendel, M. (2024). Neuronal and oligodendroglial, but not astroglial, tau translates to in vivo tau PET signals in individuals with primary tauopathies. *Acta Neuropathologica*, *148*, 70. https://doi.org/10.1007/s00401-024-02834-7 (**IF: 9.3**)

4. Bartos, L. M., Kirchleitner, S. V., Kolabas, Z. I., Quach, S., Beck, A., Lorenz, J., Blobner, J., Mueller, S. A., Ulukaya, S., Hoeher, L., Horvath, I., Wind-Mark, K., Holzgreve, A., Ruf, V. C., Gold, L., **Kunze, L. H.**, Kunte, S. T., Beumers, P., Park, H. E., … Brendel, M. (2023). Deciphering sources of PET signals in the tumor microenvironment of glioblastoma at cellular resolution. *Science Advances, 9*(43), eadi8986. https://doi.org/10.1126/sciadv.adi8986 (**IF: 11.7**)
5. **Kunze, L. H.**, Ruch, F., Biechele, G., Eckenweber, F., Wind-Mark, K., Dinkel, L., Feyen, P., Bartenstein, P., Ziegler, S., Paeger, L., Tahirovic, S., Herms, J., & Brendel, M. (2023). Long-Term Pioglitazone Treatment Has No Significant Impact on Microglial Activation and Tau Pathology in P301S Mice. *International Journal of Molecular Sciences*, *24*(12), 10106. https://doi.org/10.3390/ijms241210106 (**IF: 5.6**)
6. Palumbo, G., **Kunze, L. H.**, Oos, R., Wind-Mark, K., Lindner, S., von Ungern-Sternberg, B., Bartenstein, P., Ziegler, S., & Brendel, M. (2023). Longitudinal Studies on Alzheimer Disease Mouse Models with Multiple Tracer PET/CT: Application of Reduction and Refinement Principles in Daily Practice to Safeguard Animal Welfare during Progressive Aging. *Animals*, *13*(11), 1812. https://doi.org/10.3390/ani13111812 (**IF: 3.0**)
7. van Lengerich, B., Zhan, L., Xia, D., Chan, D., Joy, D., Park, J. I., Tatarakis, D., Calvert, M., Hummel, S., Lianoglou, S., Pizzo, M. E., Prorok, R., Thomsen, E., Bartos, L. M., Beumers, P., Capell, A., Davis, S. S., de Weerd, L., Dugas, J. C., … , **Kunze, L. H.**, … , Monroe, K. M. (2023). A TREM2-activating antibody with a blood–brain barrier transport vehicle enhances microglial metabolism in Alzheimer's disease models. *Nature Neuroscience, 26*, 416–429. https://doi.org/10.1038/s41593-022-01240-0 (**IF: 21.3**)
8. Vogler, L., Ballweg, A., Bohr, B., Briel, N., Wind, K., Antons, M., **Kunze, L. H.**, Gnörich, J., Lindner, S., Gildehaus, F.-J., Baumann, K., Bartenstein, P., Boening, G., Ziegler, S. I., Levin, J., Zwergal, A., Höglinger, G. U., Herms, J., & Brendel, M. (2023). Assessment of synaptic loss in mouse models of β-amyloid and tau pathology using [^{18}F]UCB-H PET imaging. *NeuroImage: Clinical*, *39*, 103484. https://doi.org/10.1016/j.nicl.2023.103484 (**IF: 4.9**)
9. Bartos, L. M., Kirchleitner, S. V., Blobner, J., Wind, K., **Kunze, L. H.**, Holzgreve, A., Gold, L., Zatcepin, A., Kolabas, Z. I., Ulukaya, S., Weidner, L., Quach, S., Messerer, D., Bartenstein, P., Tonn, J. C., Riemenschneider, M. J., Ziegler, S., von Baumgarten, L., Albert, N. L., & Brendel, M. (2022). 18 kDa translocator protein positron emission tomography facilitates early and robust tumor detection in the immunocompetent SB28 glioblastoma mouse model. *Frontiers in Medicine*, *9*, 992993. https://doi.org/10.3389/fmed.2022.992993 (**IF: 5.1**)

Conference Abstracts

Within the scope of the investigations related to the listed publications, the data was presented at national and international conferences:

1. **Kunze, L. H.**, Palumbo, G., Wind, K., Ziegler, S., & Brendel, M. (2025). Gemeinsame Progression von fibrillärer Amyloidose, Synapsendichte und Mikrogliose im Cortex eines Amyloid-Mausmodells. *Nuklearmedizin*, *64*. https://doi.org/10.1055/s-0045-1804287

2. Li, Y., **Kunze, L. H.**, Palumbo, G., Lindner, S., Gildehaus, F. J., & Brendel, M. (2025). Longitudinal synaptic density assessment in a tau pathology model: An [18F] UCB-H PET imaging study. *Nuklearmedizin*, *64*. https://doi.org/10.1055/s-0045-1804356
3. Thevis, J., **Kunze, L. H.**, Härtel, M., Fuxjäger, I. S., Park, H. E., Li, Y., Wind, K., Palumbo, G., Oos, R., von Baumgarten, L., Bartos, L., & Brendel, M. (2025). Vergleichende Bildgebung des Glioblastom (SB28) zwischen [18F]FET-PET und [18F]D2-Deprenyl-PET im Mausmodell. *Nuklearmedizin*, *64*. https://doi.org/10.1055/s-0045-1804355
4. Gnörich, J., Slemann, L., Hummel, S., Bartos, L., Klaus, C., Kunte, S., **Kunze, L.**, Englert, A., Katzdobler, S., Palleis, C., Beyer, L., Van Eimeren, T., Drzezga, A., Sabri, O., Barthel, H., Respondek, G., Levin, J., Höglinger, G., Herms, J., … Brendel, M. (2024). Neuronal but not Astrocytic Tau Dominates the Signal Source of in vivo PET Signaling in 4-Repeat Tauopathies. *European Journal of Nuclear Medicine and Molecular Imaging*, *51 (Supplement 1)*. https://doi.org/10.1007/s00259-024-06838-z
5. **Kunze, L.**, Palumbo, G., Wind-Mark, K., Messer, J., Ziegler, S., Brendel, M., & Lindemann, L. (2024). Fibrillar amyloidosis and synaptic vesicle protein expression progress jointly in the cortex of a mouse model with β-amyloid pathology. *European Journal of Nuclear Medicine and Molecular Imaging*, *51 (Supplement 1)*. https://doi.org/10.1007/s00259-024-06838-z
6. Park, H., Hoermann, L., **Kunze, L. H.**, Kirchleitner, S. V., Müller, K. J., Von Baumgarten, L., Albert, N. L., Brendel, M., & Bartos, L. M. (2024). Vergleich zweier immunsupprimierter Mausmodelle bezüglich des Imaging Phänotyps eines murinen Glioblastoms. *Nuklearmedizin*, *63*. https://doi.org/10.1055/s-0044-1782339
7. Englert, A., Slemann, L., Hummel, S., Hörmann, L., **Kunze, L.**, Palleis, C., Wind-Mark, K., Lindner, S., Bartenstein, P., Ziegler, S., Albert, N., Levin, J., Brendel, M., & Gnörich, J. (2023). Applicability of early phase imaging with 18F-PI-2620 and 18F-Florbetaben in mouse models with Tau and Amyloid pathology. *European Journal of Nuclear Medicine and Molecular Imaging*, *50 (Supplement 1)*. https://doi.org/10.1007/s00259-023-06333-x
8. **Kunze, L.**, Wind, K., Palumbo, G., Bartenstein, P., Ziegler, S., Honer, M., Rodriguez Sarmiento, R., & Lindemann, L. (2023). Direct competition binding between a vesicle glycoprotein 2A (SV2A) PET ligand and a γ-secretase-modulator tool compound. *The Journal of Nuclear Medicine*, *64 (Supplement 1)*.
9. Hummel, S., Dinkel, L., Bartos, L. M., Wind-Mark, K., Slemann, L., **Kunze, L.**, Englert, A., Hoermann, L., Gnörich, J., Lindner, S., Bartenstein, P., Albert, N. L., Brendel, M., & Tahirovic, S. (2023). Specific NPC1 loss in microglia of the mouse brain leads to neuroinflammation and results in synaptic loss. *Nuklearmedizin*, *62*. https://doi.org/10.1055/s-0043-1766198
10. Englert, A. L., Bartos, L. M., Palleis, C., Hummel, S., Hoermann, L., Schlaphoff, L., **Kunze, L. H.**, Gnörich, J., Wind-Mark, K., Lindner, S., Bartenstein, P., Simons, M., Ziegler, S., Albert, N. L., Levin, J., & Brendel, M. (2023). Microglia drive TSPO PET signal increases in a tauopathy mouse model. *Nuklearmedizin*, *62*. https://doi.org/10.1055/s-0043-1766199
11. **Kunze, L. H.**, Ruch, F., Biechele, G., Eckenweber, F., Wind-Mark, K., Feyen, P., Bartenstein, P., Ziegler, S., Paeger, L., Herms, J., & Brendel, M. (2023). Pioglitazone does not modulate microglia activation in P301S mice. *Nuklearmedizin*, *62*. https://doi.org/10.1055/s-0043-1766346

12. Bartos, L., Kirchleitner, S., Blobner, J., Wind, K., Holzgreve, A., Gold, L., **Kunze, L.**, Antons, M., Kunte, S. T., Beumers, P., Quach, S., Messerer, D., Bartenstein, P., Tonn, J. C., Von Baumgarten, L., Riemenschneider, M. J., Albert, N. L., & Brendel, M. (2022). Tumor cells drive 18 kDa translocator protein (TSPO) PET tracer signals of experimental and clinical glioblastoma. *European Journal of Nuclear Medicine and Molecular Imaging*, *49 (Supplement 1)*. https://doi.org/10.1007/s00259-022-05924-4
13. Hummel, S., Dinkel, L., Bartos, L., Wind, K., Sebastian Monasor, L., Slemann, L., **Kunze, L.**, Gnörich, J., Lindner, S., Bartenstein, P., Albert, N., & Brendel, M. (2022). Specifc loss of NPC1 in myeloid cells drives single cell 18kDa translocator protein expression in microglia and leads to reactive astrocytosis and loss of synaptic function. *European Journal of Nuclear Medicine and Molecular Imaging*, *49 (Supplement 1)*. https://doi.org/10.1007/s00259-022-05924-4
14. Eckenweber, F., Eyring, L., Krammer, S., Krammer, C., Li, Y., Jakob, N., Köhler, M., **Kunze, L.**, Wind, K., Beyer, L., Biechele, G., Lindner, S., Gildehaus, F. J., von Ungern-Sternberg, B., Ziegler, S., Boening, G., Baumann, K., Herms, J., Bartenstein, P., & Brendel, M. (2022). Artificial Intelligence for early identification of Amyloid positivity in transgenic Alzheimer mice. *Nuklearmedizin*, *62*. https://doi.org/10.1055/s-0042-1745971
15. Hummel, S., Slemann, L., Gnoerich, J., **Kunze, L. H.**, Biechele, G., Sanchez, P. E., Haass, C., Bartenstein, P., Ziegler, S., Monroe, K. M., Willem, M., & Brendel, M. (2022). F-18-florbetaben-PET shows distinct distribution patterns of β-amyloid in different knock-in AD mouse models. *Nuklearmedizin*, *62*. https://doi.org/10.1055/s-0042-1746038

Zusammenfassung

Hintergrund

Obwohl die Alzheimer-Erkrankung (Alzheimer's disease, AD) ein großes gesundheitliches Problem für die Bevölkerungsgruppe über 65 Jahren darstellt, konnten die zugrundeliegenden pathologischen Mechanismen noch nicht abschließend geklärt werden und es handelt sich weiterhin um eine unheilbare Erkrankung. In der Forschung werden Tiermodelle genutzt, um das Verständnis der Hintergründe der Erkrankung weiter voranzubringen. Im Einklang mit der Amyloid-Hypothese, die die Ablagerungen von Amyloid-β (Aβ) als primären Krankheitsauslöser betrachtet, werden Amyloid-Mausmodelle als besonders wertvoll zur Erforschung von AD angesehen. Weiterhin bietet die Positronen-Emissions-Tomographie (PET) die einzigartige Möglichkeit, den Erkrankungsverlauf longitudinal in diesen Mausmodellen zu beobachten, wobei zusätzlich auch die Anzahl der benötigten Tiere für eine Studie verringert wird.

Ziel

Das Ziel dieser Doktorarbeit ist es, neue Erkenntnisse zu dem Verlauf der neuropathologischen Kennzeichen von AD zu liefern. Dabei liegt der Fokus auf der mittels PET gemessenen Aβ-Akkumulation, der Neuroinflammation und der Synapsendichte in zwei Amyloid-Mausmodellen. Somit konnte gezeigt werden, wie sich Merkmale der AD typischen Pathologie mittels der nichtinvasiven PET-Bildgebung durch verschiedene Radiotracer darstellen und im longitudinalen Verlauf über sechs Monate in den APPSL70 und über 15 Monate im APP^{SAA} Mausmodell verfolgen lassen können.

Material und Methoden

Erste Publikation

APPSL70 und C57Bl/6 Mäuse erhielten longitudinale PET-Scans über einen Zeitraum von sechs Monaten zur Messung der Aβ-Akkumulation, Synapsendichte und Neuroinflammation. Mittels statistical parametric mapping (SPM) wurden Gruppenunterschiede in der dreidimensionalen Tracerverteilung gemessen. Ähnlichkeiten zwischen diesen Verteilungen wurden mit dem Dice-Koeffizienten berechnet. Die Ergebnisse der PET-Studie wurden durch immunhistochemische Färbungen validiert.

Zweite Publikation

Zur Charakterisierung des neuartigen Amyloid-Mausmodells, welches die Schwedische, Arktische und Österreichische Mutation trägt, wurde mittels biochemischer und immunhistochemischer Methoden, PET-Bildgebung und weiterer bildgebender Verfahren, sowie Verhaltenstests die Aβ-Akkumulation, Neurodegeneration und Neuroinflammation bis zum Alter von 23 Monaten gemessen.

Ergebnisse

Erste Publikation

Der Hypothalamus wurde als passende Referenzregion für alle vier Tracer identifiziert. Wir fanden einen Anstieg der Expressionslevel des synaptisches Vesikelproteins 2A (SV2A), der zeitlich und örtlich mit einem parallelen Anstieg der Amyloidose im APPSL70 Mausmodell verbunden war. Weiterhin war dieser Prozess mit einem Anstieg der Mikrogliaaktivierung verbunden. SPM Bilder aller drei Tracer wiesen eine hohe Ähnlichkeit der Bindungsmuster auf, was ein Dice-Koeffizient von 53 % bzw. 58 % nochmals unterstreicht. Im Gegensatz dazu war eine Reaktivität der

Astrozyten nicht an die SV2A Expression gekoppelt. Immunhistochemische Färbungen validierten die PET-Ergebnisse.

Zweite Publikation

Wir haben ein neues *App* knock-in Mausmodell (APP^{SAA}) etabliert und charakterisiert. Während die Expressionslevel des Amyloid-Precursor-Proteins (APP) nicht verändert waren, war das Aβ1-42/1-40 Verhältnis erhöht, was zu einer Amyloid-Plaque Ablagerung ab einem Alter von vier Monaten führte. Zusätzlich wurden Anzeichen von Neurodegeneration in Form von dystrophischen Neuriten und einem erhöhten Spiegel von neurofilament light chain (NfL) im Liquor gefunden. Weiterhin konnte man mittels PET-Bildgebung eine ausgedehnte Inflammation und einen erhöhten Glukosemetabolismus in den APP^{SAA} Mäusen feststellen. In den Verhaltenstest wurde ein hyperaktiver Phänotyp festgestellt.

Schlussfolgerung

Mausmodelle sind ein wichtiges Werkzeug, um die pathologischen Veränderungen von neurodegenerativen Erkrankungen zu untersuchen. Hierfür kann das neue APP^{SAA} Mausmodell neue Einblicke gewähren, während damit Artefakte, die einer übermäßigen Expression des APPs geschuldet sind, vermieden werden. Zusätzlich ist die PET-Bildgebung von Neuroinflammation, Aβ Akkumulation und Synapsendichte eine nützliche Methode, um die Verbindung von verschiedenen pathologischen Veränderungen zu verstehen. So argumentieren wir, dass der Anstieg der SV2A Expressionslevel im APPSL70 Mausmodell wahrscheinlich ein kompensatorischer Mechanismus in Reaktion auf die Proteinakkumulation ist. Unsere Ergebnisse ergänzen die bisherigen Forschungsergebnisse, die einen Glukose-Hypermetabolismus in verschiedenen Amyloid-Mausmodellen, unter anderem dem APP^{SAA} Mausmodell, gezeigt haben. Statt diesen lediglich einer erhöhten Immunantwort zuzuschreiben, vermuten wir aufgrund des SV2A-Anstiegs einen Zusammenhang des Hypermetabolismus mit einer Hyperexzitabilität von neuronalen Zellen in den Frühstadien von AD.
Zusammenfassend lässt sich sagen, dass bei der Untersuchung der pathologischen Veränderungen bei AD und der Behandlung der Erkrankung mit geeigneter Therapie noch vor dem Einsetzen von irreversibler Neurodegeneration, die Forschung an Mausmodellen wie dem APP^{SAA} Mausmodell und passenden Techniken wie der PET-Bildgebung ein Schlüsselelement darstellt.

Abstract

Background

Although Alzheimer's disease (AD) is a major health problem especially in the elderly population, the exact pathological mechanisms could not be unraveled yet and we are still lacking a cure. Research uses animal models to enhance the understanding of the underlying pathology of AD. In line with the amyloid cascade hypothesis that assumes the aggregation of amyloid-β (Aβ) as primary cause for the disease, mouse models of amyloidosis are especially valuable for this purpose. In addition, the use of positron emission tomography (PET) provides the unique opportunity to longitudinally monitor the disease progression in these models, thereby also reducing the number of animals needed in one study.

Aim

The aim of this thesis is to provide novel insights into the trajectories of neuropathological hallmarks of AD, focusing on Aβ deposition, neuroinflammation, and synaptic density, by evaluating the results of longitudinal PET imaging in two amyloidosis mouse models. Thus, it could be shown how the pathological hallmarks of AD can be visualized and longitudinally followed for six months in the APPSL70 and 15 months in the APP^{SAA} mouse model with non-invasive PET imaging using different radiotracers.

Materials and Methods

First publication

APPSL70 and C57Bl/6 mice underwent longitudinal PET imaging over a period of six months for Aβ accumulation, synaptic density, and neuroinflammation. Statistical parametric mapping (SPM) was used to assess group level differences between the three-dimensional distribution of the tracers. Similarity of these distribution patterns were assessed with the dice coefficient. The results from the PET study were validated with immunohistochemical stainings.

Second publication

The characterization of the novel amyloidosis mouse model harboring the Swedish, Arctic, and Austrian mutation was achieved with different biochemical, immunohistochemical, PET imaging, and other imaging techniques, as well as behavioral tests, to assess Aβ accumulation, neurodegeneration, and neuroinflammation up to an age of 23 months.

Results

First publication

We identified the hypothalamus as suitable reference region for all four tracers. Furthermore, we saw a spatially and temporally connected rise in the synaptic vesicle protein 2A (SV2A) expression levels and amyloidosis in the APPSL70 mouse model. This progress was accompanied by a similar rise in microglial activation and all three tracers showed a similar spatio-temporal agreement in SPM images, as shown with a Dice coefficient of 53 % and 58 %, respectively. In contrast, astrocytic reactivity was unrelated to SV2A expression levels. Immunohistochemical stainings confirmed the observed PET results.

Second publication

We established and characterized a novel *App* knock-in mouse model (APP^{SAA}). It was shown that while the expression of the amyloid precursor protein (APP) was not changed, the

Aβ1-42/1-40 ratio was increased, leading to amyloid plaque deposition starting from four months of age. In addition, characteristic features of neurodegeneration, namely dystrophic neurites and increased neurofilament light chain (NfL) cerebrospinal fluid (CSF) levels, were found. Moreover, PET measurements revealed a widespread inflammation and an increased glucose metabolism in the APP^{SAA} mice. In the behavior tests, the mice presented a hyperactive phenotype.

Conclusion

Mouse models are an important tool to investigate the pathological changes of neurodegenerative diseases. Therefore, the new APP^{SAA} mouse model can provide novel insights, thereby avoiding potential artefacts introduced by an APP overexpression. In addition, PET imaging of neuroinflammation, Aβ accumulation, as well as synaptic density is a useful tool to understand the connection between several pathological changes. Likewise, we argue that the increase in SV2A expression levels in the APPSL70 mouse model is likely a compensatory mechanism reacting on the protein accumulation. Our findings add to the observed glucose hypermetabolism in previous preclinical studies with amyloidosis mouse models, including the APP^{SAA} mice, ascribing this phenomenon not only to an increased inflammatory response but also in the light of a rise in SV2A expression levels proposing a connection with measured hyperexcitability of neuronal cells in the early stages of AD.

Concluding, to further explore the pathological features of AD and to prevent the disease by appropriate treatment before the onset of irreversible neurodegeneration, the research on animal models like the APP^{SAA} with suitable techniques like PET imaging poses a key element.

1. Contributions to Publications

1.1 Contribution to the First Publication

For the first publication, I was executing all experiments mentioned in the study and I performed all data analysis. In addition, I was responsible for caring for the animals, including daily check-ups as well as the mandatory scoring twice a week.

For the experiments, I was involved in planning all PET scans with [^{18}F]UCB-H, [^{18}F]FBB, [^{18}F]GE-180, and [^{18}F]F-DED. In addition, for each PET scan, the animals needed to be prepared for the imaging procedure, which included appropriate anesthesia with isoflurane and the insertion of a catheter into the tail vein. For [^{18}F]FBB, [^{18}F]GE-180, and [^{18}F]F-DED, the tracer was injected and imaging was conducted at the Mediso nanoScan PET/CT at tracer-specific time points after sufficient tracer uptake to the brain. For [^{18}F]UCB-H, tracer injection occurred when imaging was started to uncover the uptake kinetics of this tracer. Afterwards, I reconstructed the scans with specified parameters and I analyzed the resulting images using PMOD (version 3.5, PMOD Technologies, Zurich, Switzerland). Therefore, they were spatially normalized by matching the computer tomography (CT) to a previously designed template. Continuing spatial differences were accounted for by co-registering each PET scan to the average image of the first time point of each tracer that was created purely for this study. To normalize for variability in the images, different normalization methods were compared against each other. For all tracers, I identified the hypothalamus as a suitable reference region with no statistically significant differences across genotypes. Thus, all data was normalized to the hypothalamus. In addition, volume of distribution (V_T) images were created for [^{18}F]UCB-H with a self-defined volume of interest (VOI), namely a 2.5 mm sphere in the heart, to assess the image derived input function (IDIF). After normalization, I chose the cortical, hippocampal, and thalamic VOI of the Mirrione Atlas as target regions as these are brain regions particularly affected by AD.

In addition, SPM (*SPM12*, 2016) was performed in Matlab (*MATLAB*, 2016) to unravel group differences between C57Bl/6 and APPSL70 mice in the distribution of the tracers. To assess the similarity between tracers, I calculated the dice coefficient using a publicly available Matlab script (https://github.com/rordenlab/spmScripts/blob/master/nii_dice.m) for the SPM images of all tracers in comparison to the SPM image of [^{18}F]UCB-H.

After the last PET scan, mice were perfused and one hemisphere of the brain was harvested for immunohistochemistry. Therefore, the tissue was prepared accordingly by fixation in 4 % paraformaldehyde (PFA) and the brain was cut in 50 µm slices.

Furthermore, I established an immunohistochemical staining with markers for neurons (NeuN), Aβ (NAB228), and synapses (SV2A). After determination of the most suitable antibodies, imaging was conducted on the THUNDER Imager Tissue (Leica Microsystems CMS GmbH, Wetzlar, Germany) with a x63 oil objective by acquiring z-stacks of 10 µm. I was responsible for establishing the equipment and procedures of the microscopic analysis. The respective immunohistochemical images were prepared for analysis by creating a maximum projection of the z-stacks. The analysis was carried out with ImageJ (Schindelin et al., 2012). While the parameters were defined manually, the process of analysis was accelerated by a self-written script.

All data, PET as well as immunohistochemistry, were statistically assessed using GraphPad Prism (version 9.5.1 for Windows, GraphPad Software, San Diego, CA, USA). The data was interpreted and put in context with the previous research. Afterwards, I was compiling the results

by writing the original draft of the manuscript, reviewing and editing the manuscript before publication, and I created a graphical abstract to display the research.

1.2 Contribution to the Second Publication

In the scope of the second publication, I participated in the PET imaging study. Therefore, I was involved in planning the scans in accordance with the radiochemistry and the availability of the Mediso nanoScan PET/MR 3T. Then, the animals were prepared for the imaging, which included fasting before the [^{18}F]FDG-PET scans as well as insertion of a catheter to the tail vein of the mice under anesthesia with isoflurane.

It was of particular importance to adjust the anesthesia to the model to reduce the mortality of the mice. For that purpose, I designed a new anesthesia chamber, facilitating the preparation of the animals before the PET scans.

Furthermore, we injected the respective radioactive tracer, namely [^{18}F]GE-180 for translocator protein (TSPO) imaging of activated microglia and [^{18}F]FDG for imaging of the glucose metabolism. The PET scans were performed at tracer-specific time points, yielding an optimized uptake of the tracer to the brain. Afterwards, the images were reconstructed with suitable parameters and analyzed using PMOD (version 3.5, PMOD Technologies, Zurich, Switzerland).

Moreover, I took part in the data analysis. Therefore, the reconstructed images were spatially normalized to a standardized PET template specific to each tracer. I furthermore participated in critically reviewing the scans to uncover any methodological or technical difficulties and to ensure data integrity. After testing multiple normalization approaches of the three-dimensional distribution of the tracers to account for differences in the injected activity and the weight of the mice, we decided on calculating a standardized uptake value (SUV) for the [^{18}F]FDG-PET data and the previously described myocardial correction for the [^{18}F]GE-180-PET data. A cortical VOI was used to assess the differences in the mouse models in a region that is particularly affected by changes in amyloidosis mouse models.

The results were then statistically quantified and interpreted regarding the results of the other techniques, which resulted in a comprehensive figure and the description of the results in the final paper.

2. Introduction

2.1 Alzheimer's Disease

AD is among the leading causes of death (Alzheimer's Association, 2024) accounting for 84 446 deaths in the European Union in 2021 (Eurostat, 2025). It is by far the form of dementia most people (60-80 %) are suffering from (Alzheimer's Association, 2024; Förstl et al., 2020) and it is estimated that approximately 416 million people above the age of 50 show signs of AD, most of them being in the asymptomatic, preclinical phase, while, roughly estimated, 32 million people worldwide are demented AD patients (Gustavsson et al., 2023). With the number of people newly diagnosed for dementia likely to double by 2050 (Alzheimer's Association, 2024), AD poses a major health-care problem that will worsen with the demographic change in the population, as age is the major risk factor for AD (Alzheimer's Association, 2024; Förstl et al., 2020). In Germany, hospitalizations due to AD rose by nearly 61 % from 2003 to 2022, while deaths due to AD were doubling within the same time (Statistisches Bundesamt (Destatis), 2024). Thus, AD and related dementias pose a monetary burden together with social and psychological implications for patients and caregivers (Alzheimer's Association, 2024; Statistisches Bundesamt (Destatis), 2025).

Clinical symptoms of AD are diverse, depending on the area of the brain being mostly affected, but usually consist of memory impairments, including the inability to recognize loved ones, disturbances in language skills and orientation, personality changes and mood swings, and losing control over bodily functions such as bladder control (Förstl et al., 2020). While there are symptomatic treatment options available, only two drugs are currently targeting the underlying pathology of the disease (see section 2.1.4.) that is known to start decades before the clinical onset of AD (Jack Jr. et al., 2024; Khan & Graff-Radford, 2017; Rabinovici et al., 2025; Sperling et al., 2011). Before symptoms become apparent, patients are in the so-called preclinical phase, where biomarkers for AD are already building up and can be detected by PET measurements or blood and CSF tests (see section 2.1.3.), but do not have an impact on the patient's daily life. When first subtle symptoms are arising, patients transition into mild cognitive impairment (MCI), however, this does not interfere with daily activities. For an estimated one-third, symptoms worsen within the next five years and they can be diagnosed with dementia due to AD that is progressively worsening and divided into a mild, moderate, and severe AD (Alzheimer's Association, 2024).

2.1.1 Molecular Background of Alzheimer's Disease

Already at the beginning of the 20th century, Alois Alzheimer described the main hallmarks of Alzheimer's disease, namely neurodegeneration, extra- and intracellular protein aggregation, and neuroinflammation (Alzheimer, 1911). While at that time, the origin of these hallmarks could not be clarified yet (Alzheimer, 1911), a large amount of research was conducted to define the pathological background of AD.

The most striking hallmark of AD is the disturbance of neurons and synapses, ultimately leading to synaptic and neuronal loss and consequently brain atrophy. This degeneration is accountable for the continuously worsening cognitive ability of the patients, ultimately being fatal for the affected (Davies et al., 1987; Lichtenthaler, 2017; Tai et al., 2021; Terry et al., 1991; Wolfe, 2021). Before neurodegeneration sets in, the hampered neuronal signaling manifests in a state of hyperexcitability that might lead to increased epileptic seizures patients are experiencing in the early stages of the disease (Busche et al., 2008; Mao et al., 2024; Vossel et al., 2013).

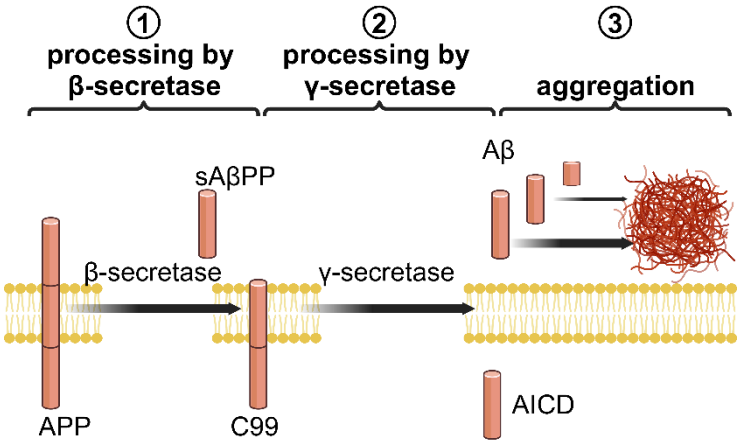

Figure 1 Processing of APP by β- and γ-secretase resulting ultimately in Aβ fragments with longer fragments tending to aggregate to Aβ plaques comprising a major hallmark of AD. APP = amyloid precursor protein, sAβPP = soluble amyloid-β precursor protein, C99 = C-terminal fragment 99, AICD = Amyloid Intracellular Domain, Aβ = Amyloid-β

On the cellular level, pathological changes occur years before the actual symptom onset (Jack Jr. et al., 2024; Khan & Graff-Radford, 2017; Lichtenthaler, 2017; Rabinovici et al., 2025; Sperling et al., 2011; Tai et al., 2021). Intracellularly, misfolded phosphorylated tau is accumulating, thus disturbing the transport of molecules within the cell and hampering the synaptic connections of neurons (Förstl et al., 2020). Extracellularly, polymers of the APP, namely Aβ peptides, are accumulating to Aβ plaques (Cohen et al., 2019). APP is a ubiquitously expressed membrane-spanning protein that can be processed in different ways. Relevant for AD is the processing by the enzymes β-secretase and γ-secretase (**Figure 1**). Processing of APP by the former gives rise to the membrane-bound fragment C99. This protein is further cut by the γ-secretase into fragments of different lengths, with more cuts leading to shorter fragments, which are then released into the extracellular space (Haapasalo & Kovacs, 2011; Voytyuk et al., 2018). Longer fragments, namely Aβ1-42 and Aβ1-43, are more prone to aggregate into the characteristic Aβ plaques (Haapasalo & Kovacs, 2011; Voytyuk et al., 2018). The plaques might then impede the neuronal communication, ultimately leading to neuronal damage (Busche et al., 2008).

Alzheimer's disease further includes inflammatory processes in the brain with activated microglia and reactive astrocytes (Ballweg et al., 2023; Peretti et al., 2024; Sebastian Monasor et al., 2020; Tai et al., 2021). It is controversial, however, if the immune response is a rather positive process, removing the protein accumulation to protect the neuronal tissue (Bolós et al., 2016; Ewers et al., 2020), or has mainly negative effects (Fakhoury, 2018; Wolf et al., 2017). Especially astrocytes are involved in a wide variety of functions, including being involved in the neuronal metabolism, forming the blood-brain barrier, inflammation and protein degradation, and neuronal signaling by their participation in especially excitatory neurotransmission (Carter et al., 2019). In that regard, chronic inflammation by microglia and astrocytes might be destructive and could lead to scar formation, impaired neuronal signaling, and metabolic dysfunctions, both adding and accelerating the neurodegenerative processes (Acioglu et al., 2021; Eckenweber et al., 2020; Hickman et al., 2008; Olsen et al., 2017; Peretti et al., 2024).

While the major risk factor for Alzheimer's disease is old age, there are also rare cases of familiar AD, where genetic predispositions are autosomal dominantly passed onto the offspring. Familiar AD is accountable for less than 1 % of AD cases and a result of mutations in either the *APP* gene or genes encoding for two parts of the γ-secretase enzyme, namely presenilin 1 (*PSEN1*) and presenilin 2 (*PSEN2*) (Alzheimer's Association, 2024; Förstl et al., 2020; Yokoyama et al., 2022). A more common genetic risk factor is the expression of apolipoprotein E ε4 (*APOE4*), which is involved in the lipid transport, especially interacting with very low density lipoproteins (VLDLs). Its exact role in AD through e.g. blood-brain-barrier disruption, protein aggregation, as well as effects on neuronal signaling is intensely discussed (Förstl et al., 2020; Gustavsson et al., 2023; Huang & Mahley, 2014). It increased the risk to experiencing dementia by 80 years of age from being 5-

7 % for non-carriers of the ε4 isoform to 31-40 % for people carrying two copies of this isoform (Chatterjee et al., 2023; Qian et al., 2017).

2.1.2 Animal Models for Alzheimer's Disease Pathology

As mice naturally do not develop AD, numerous animal models are genetically modified to enable the characteristic tau or Aβ accumulation, thereby relying on the genetic predispositions that make a person susceptible to develop the disease (Tai et al., 2021). Following the amyloid cascade hypothesis claiming that the pathological aggregation of Aβ fragments is the primary cause of AD (Hardy & Higgins, 1992), the majority of research models is concerned with alterations of APP and its processing enzymes, β- and γ-secretase. An insertion of a specific gene can be achieved by making use of homologous recombination, a mechanism responsible for repairing DNA breaks as well as leading to a higher genetic variance by exchanging maternal and paternal chromosomal information during meiosis, thus leading to new unique genetic combinations (Alberts et al., 2022a). Examples of amyloidosis mouse models harboring genetic APP mutations would be the APPSL70 mouse model used in the first publication and the APP^{SAA} mouse model used in the second publication. The former is harboring the Swedish and London mutation, both increasing the production of Aβ fragments (Eckman et al., 1997; Goate et al., 1991; Mullan et al., 1992; Yokoyama et al., 2022). The latter is harboring the Swedish, Arctic, and Austrian mutation (Xia et al., 2022), leading to an increased production of Aβ fragments and a higher tendency for these fragments to aggregate (Kumar-Singh et al., 2000; Mullan et al., 1992; Nilsberth et al., 2001; Yokoyama et al., 2022). These mutations lead to a measurable Aβ deposition at four months of age for the APP^{SAA} and congophilic plaques in five to six months old APPSL70 mice, together with other hallmarks of AD like neuroinflammation (Blume et al., 2018; Xia et al., 2022). While animal models cannot fully reflect the human pathology, they can nonetheless provide valuable insights into the mechanisms behind AD pathobiology, further enhancing our understanding of the disease (Tai et al., 2021; Yokoyama et al., 2022).

2.1.3 Diagnosis of Alzheimer's Disease

AD used to be mainly diagnosed by assessing the clinical symptoms, namely memory dysfunction and behavioral changes (Dubois et al., 2023; Förstl et al., 2020). However, defining the disease based on clinical criteria alone has proven to be insufficient (Beach et al., 2012). Recently, the National Institute on Aging and the Alzheimer's Association suggested a more biologically driven diagnosis based on pathological changes rather than their symptomatic expression (Jack Jr. et al., 2024). Thus, blood- and CSF-based biomarkers as well as PET imaging play an important role in the identification of AD patients. Thereby, amyloid PET is considered sufficient alone to diagnose a patient with Alzheimer's disease (Jack Jr. et al., 2024). The Alzheimer's Association together with the Society of Nuclear Medicine and Molecular Imaging has released guidelines helping physicians to decide on whether an amyloid or tau PET scan is appropriate. Likewise, they mention cases where the diagnosis supported by PET can have an influence on patient treatment, making it a crucial addition to the diagnostic procedure (Rabinovici et al., 2025).

Blood- and CSF-based biomarkers include abnormal levels of Aβ1-42 or a change in Aβ1-42/1-40 ratio, phosphorylated tau species, as well as markers of neuroinflammation like glial fibrillary acidic protein (GFAP), and neuronal death like NfL (Chatterjee et al., 2023; Dubois et al., 2023; Jack Jr. et al., 2024). Yet, there are limitations to the use of biomarkers as diagnostic tools for AD. Thus, a positive AD related biomarker should be interpreted in the scope of the patient's individual features. For example, at 65 years of age, around one fifth of the people with unimpaired

cognition were observed to have a positive amyloid PET scan and amyloid abnormalities in the CSF, which are values only slightly lower compared to people with subjective cognitive decline. These values increased to approximately half of the cognitively normal individuals showing an amyloid positivity in PET and CSF at 85 years of age (Jansen et al., 2022). Accordingly, diagnosis should be performed considering both, neuropathological biomarkers as well as the clinical presentation (Jack Jr. et al., 2024). Thus, although blood-based biomarkers would provide a cost-efficient and little invasive measure of AD diagnosis and progression, an approval for clinical use is still lacking (Rabinovici et al., 2025).

2.1.4 Current Treatment of Alzheimer's Disease

Treatment of AD includes regulation of the neuronal signaling by cholinesterase inhibitors and medication regulating glutamatergic transmission, and psychotherapeutic approaches as well as antidepressants for behavioral changes (Förstl et al., 2020; Yiannopoulou & Papageorgiou, 2020). In 2021, the anti-amyloid antibody aducanumab (Budd Haeberlein et al., 2022) was approved by the FDA in a controversially discussed expedited procedure, providing a first disease-modifying treatment. Recently, another anti-amyloid antibody, lecanemab, showed promising results in slowing the rate of cognitive decline (van Dyck et al., 2023). It was approved by the FDA in 2023 and by the European Commission in April 2025. Further ongoing research includes modulating of the γ-secretase, inducing neurotrophic factors, and immunomodulation (Fakhoury, 2018; Heneka et al., 2005; Nasrolahi et al., 2022; Ratni et al., 2020; Yiannopoulou & Papageorgiou, 2020).

2.2 Objective of this Thesis

The objective of this thesis is to evaluate different pathological hallmarks of AD in two amyloidosis mouse models, namely the newly characterized APP^{SAA} and the already described APPSL70 mouse model, providing novel insights into the pathobiology of AD. To this end, it is shown that biomarkers of neurodegenerative diseases, as displayed in mouse models of AD, can be measured longitudinally with PET imaging (**Figure 2**).

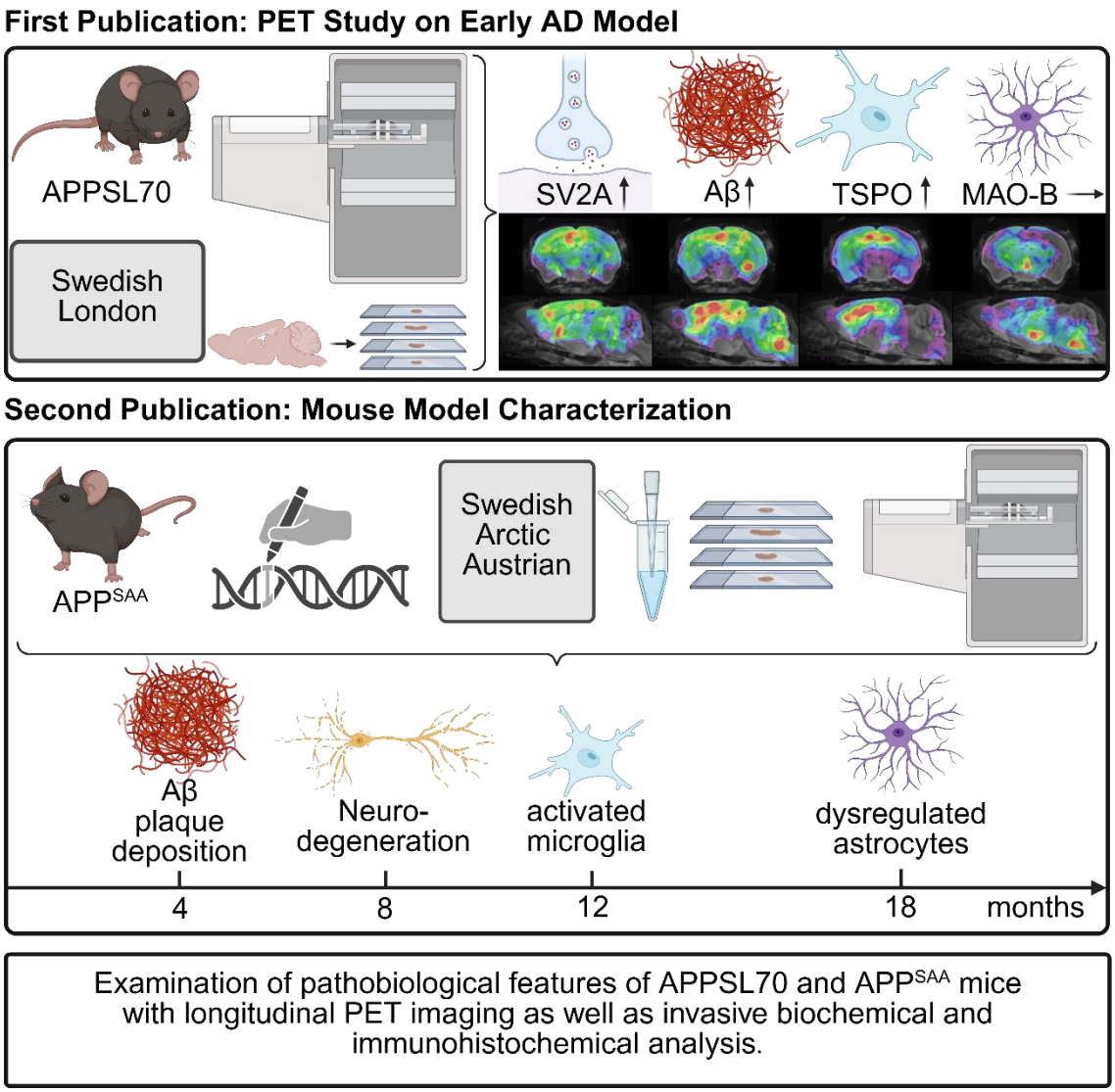

Figure 2 Objective of the Thesis: Examination of Aβ plaque deposition, neurodegeneration, and neuroinflammation in two amyloidosis mouse models. The first publication is a longitudinal PET study on APPSL70 mice, a mouse model with limited neurodegeneration. Validation of PET results was performed with immunohistochemical stainings. The second publication is concerned with the characterization of the APP^{SAA} mouse model using longitudinal PET imaging as well as biochemical techniques, immunohistochemical stainings, and behavioral tests.

3. Methods

3.1 Positron Emission Tomography

Atoms consist of a nucleus made of protons and neutrons, which is surrounded by electrons. Attractive and repulsive forces between the protons and neutrons in the nucleus are balancing the nucleus of the atom. Thus, an excessive amount of protons or neutrons results in instability of the nucleus. As all atoms strive to obtain a stable state, this instability leads to some form of radioactive decay. If there is an excessive amount of protons within the nucleus, this radioactive decay occurs in the form of β^+-decay that can be captured by PET imaging. Thereby, the excessive proton is ejecting a positron with a certain energy to convert into a neutron. After losing its remaining energy, the positron interacts with a nearby electron in a reaction named annihilation. In this process, the masses of the two particles are converted into two 511 keV photons that are emitted at an angle of 180° from each other. The number of such decays per second is described by the activity that is measured in Becquerel (Bq) (Bailey et al., 2014; Cherry & Dahlbom, 2006).

$$Activity\ [A] = 1\ Bq = \frac{1\ decay}{1\ second}$$

A common example for a radioisotope decaying in the described fashion is ^{18}F. Its physical half-life, thus the time to reduce its activity to half of its initial value, is dependent on the radionuclide specific decay constant λ and is 109.8 minutes for ^{18}F (Bailey et al., 2014; Zhang et al., 2025). The decay of a radionuclide at a specific time point t can be calculated with the following formula (Bailey et al., 2014):

$$A(t) = A_0 \cdot e^{-\lambda \cdot t}$$

However, in an organism, the activity concentration over time is also affected by the metabolism and excretion of the molecule labeled with the radioisotope, which is described by the biological half-life. Combining the physical and biological half-life is termed effective half-life (Bailey et al., 2014).

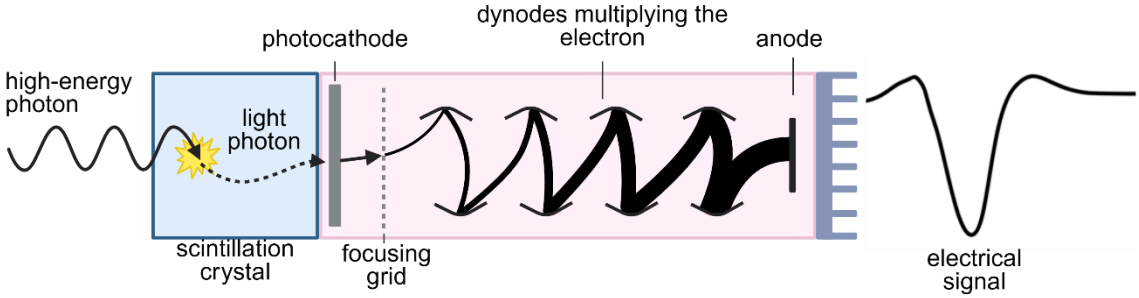

Figure 3 Schematic structure of a PET detector and the conversion of a high-energy photon into an electrical signal. Based on Bailey et al. (2014).

The high-energy photons resulting from the annihilation can be measured with a suitable detector (**Figure 3**). Such a detector consists of a scintillator material, where the energy of the high-energy photons is converted to visible light. This light is then guided to a photon detector, most often a photomultiplier tube. Inside, the photons first hit a photocathode, where they cause the emission of electrons. These electrons are then multiplied and accelerated by passing several dynodes, which results in a reinforced electrical signal. Thereby, the electrical signal is proportional to the deposited energy of the photons. In a common PET system, multiple photomultiplier tubes are

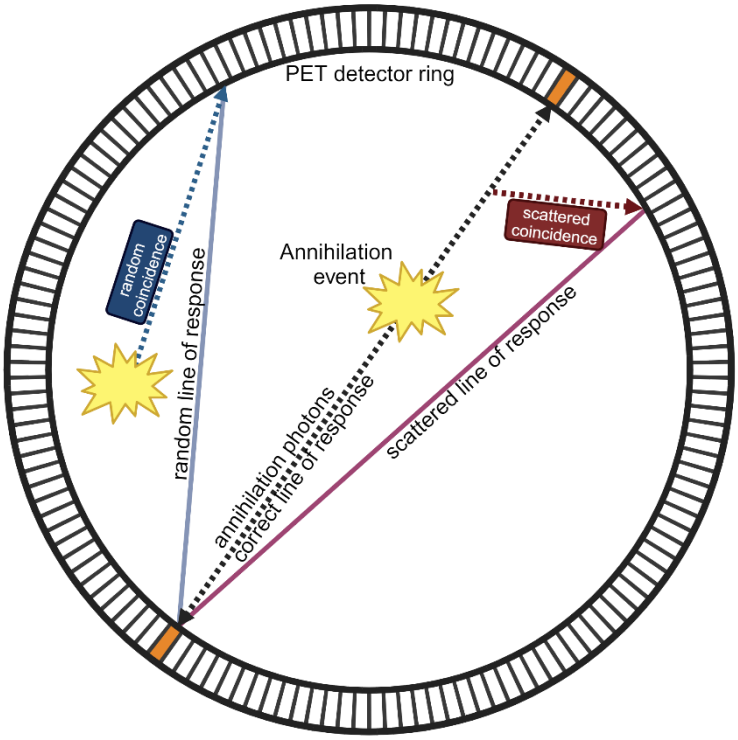

Figure 4 PET detector ring during an annihilation event. Detectors that are counting the annihilation event are highlighted in orange. Background in form of scattered coincidence (red) and random coincidences (blue).

connected to segmented scintillation crystals and multiple detectors are placed around the field of view of the system, e.g. as detector ring (Cherry & Dahlbom, 2006).

To determine the location of the annihilation, the PET system uses the Anger principle and the principle of coincidence. The former can determine the exact position the photon was hitting the scintillation crystal by making use of different signal intensities of multiple photomultiplier tubes that are connected to a segmented crystal. For the latter, only such events are considered that were detected in two opposing detectors, making use of the 180° angle emission of the 511 keV photons during annihilation. Using this coincidence detection method, the line of response where the annihilation event was taking place, can be directly determined (**Figure 4**) (Bailey et al., 2014; Cherry & Dahlbom, 2006).

The detection of the radioactive decay is disturbed by the background. Firstly, this includes scattered coincidences, where one or both of the 511 keV photons are deviating from their original path due to the interaction with the surrounding matter (**Figure 4**). Secondly, random coincidences can occur when two annihilation photons that stem from unrelated events, happen to hit a detector at the same time, thus creating an actually meaningless line of response (**Figure 4**). Thirdly, the assignment of the line of response can be hampered when multiple coincidences happen at the same time and different lines of response could be assigned to the respective annihilation photons. These events are subtracted from the total number of coincidences (Bailey et al., 2014; Cherry & Dahlbom, 2006).

The resolution and sensitivity of the PET system is further compromised by the detector response and dead time, as well as the positron range, thus the distance the positron can travel within the tissue before the annihilation event occurs. The latter is dependent on the radioisotope as well as on the tissue density (Bailey et al., 2014; Cherry & Dahlbom, 2006; Sánchez-Crespo et al., 2004).

All of these factors need to be taken into account when reconstructing an image out of the PET data as well as performing PET data analysis. One simple reconstruction method of imaging data includes the filtered backprojection (FBP), where the measured counts are simply distributed equally along the line of response (LOR) and filtered. A more flexible reconstruction method are iterative reconstructions. Thereby, a starting image is refined in multiple rounds, each time applying parameters that are accounting for image degrading effects as well as sharpening or smoothing filters that are ultimately leading to the readily reconstructed image (Bailey et al., 2014; Qi &

Leahy, 2006). For both, the Mediso nanoPET/CT and the Mediso nanoPET/MR 3T, the images were reconstructed in four iterations with a voxel size of 0.4 mm applying random, attenuation, and scatter correction, while omitting the positron range, which is, depending on the tissue, 0.2-0.8 mm in the case of ^{18}F (Sanchez-Crespo, 2013). To accelerate the reconstruction, the data was divided in six subsets. These reconstruction parameters were the same, irrespective if the PET scan was performed statically or dynamically.

Such reconstructed images were spatially normalized to a CT template for the Mediso nanoScanPET/CT scans and a PET template for the respective tracer for the Mediso nanoScanPET/MR 3T. Afterwards, the data was normalized to differences in injected activity and interindividual differences of the animals. Therefore, one of the four following methods was applied:

[^{18}F]FBB, [^{18}F]UCB-H, [^{18}F]GE-180, and [^{18}F]F-DED PET data in the first publication were corrected by calculating a standardized uptake value ratio (SUVr). Thus, a reference region that does not display any changes due to the underlying genotype of the animals was defined. The activity concentration of the target regions is then divided by the activity concentration of the reference region to account for interindividual differences like the injected activity and the distribution of the tracer within the body, and unspecific binding (Rabinovici et al., 2025). Therefore, each VOI activity concentration was divided by the activity concentration of the hypothalamus, a region that proved suitable as uniform reference for all four tracers.

As [^{18}F]UCB-H PET data in the first publication was acquired dynamically, meaning the injection of the activity occurred simultaneously with the start of the acquisition, capturing the tracer dynamics. Hence, the [^{18}F]UCB-H PET data was also corrected with an IDIF, using the blood activity levels as measured from the image to define the bound tracer activity in comparison to the unbound activity in the blood (van der Weijden et al., 2023). Therefore, a VOI is placed either in the carotid artery or, as in the first publication, in the heart to define the blood input curve. The V_T image is then calculated in PMOD using the implemented method of Logan et al. (1990).

For the [^{18}F]FDG PET data in the second publication, an SUV (Bailey et al., 2014; Mix, 2018; Pike, 2009) was calculated with the formula

$$SUV = \frac{VOI\ activity\ concentration\ value\ \cdot body\ weight\ of\ the\ animal}{injected\ activity}$$

Lastly, the [^{18}F]GE-180 PET data in the second publication was corrected for myocardial tracer uptake by subtracting a specifically calculated factor from the activity of the VOI. The myocardial correction factor is calculated with the formula

$$\begin{aligned} &myocardial\ correction\ factor \\ &= \left(\frac{activity\ concentration\ in\ the\ heart - 844.2\ \frac{kBq}{cm^3}}{273.6\ \frac{kBq}{cm^3}} \right) \cdot 44.578 \\ &+ \left(\frac{injected\ activity - 14.30\ MBq}{1.60\ MBq} \right) \cdot 9.79 \\ &+ \left(\frac{body\ weight\ of\ the\ animal - 25.4\ g}{3.7\ g} \right) \cdot (-2.4) \end{aligned}$$

To obtain this formula, Deussing et al. (2018) identified the activity concentration in the heart, the injected activity, and the body weight of the animal as the factors with the highest influence on the cerebral TSPO uptake. For each factor, the specific value of the animal is transformed into a standardized z-score that is relying on the population of animals that were assessed by Deussing

et al. (2018) and then multiplied by a therein defined regression coefficient, accounting for the respective strength of the factor's influence on the cerebral TSPO activity concentration.

3.2 Radiotracers

Radiotracers (or radiopharmaceuticals) are substances that are labelled with a radioactive isotope and that can visualize pathological and physiological changes within an organism (Schlegel et al., 2018).

3.2.1 [^{18}F]FDG

Glucose is taken up by every cell to retrieve energy necessary for the specific functions of the cell. Disturbances in the energy metabolism can be a feature of several diseases, thus making the glucose consumption visible can provide important information about the metabolic status of different tissues. To obtain an *in vivo* read-out of the energy metabolism, an analog to glucose (2-desoxy-D-glucose) was utilized, obtaining a change in structure that, while allowing it to be taken up by cells in competition with glucose, blocks its further processing and trapping it within the cell. An additional radioactive labelling then made it feasible for autoradiography and PET imaging (Ferris et al., 1980; Sokoloff et al., 1977). Still until now, the most commonly used radiotracer is the fluorine-18 labelled variant of this analog (2-[^{18}F]deoxy-2-fluoro-D-glucose or [^{18}F]fluordeoxy-glucose), which is used for a wide variety of pathologies including cancer, neurodegenerative disorders, and cardiac pathologies (Brendel et al., 2016; Ferris et al., 1980; Oh et al., 2016; Xia et al., 2022; Zhang et al., 2025). In neurodegenerative disorders, it has the capability to disclose the energy consumption of the brain, believed to be a read-out of early hyperexcitability or neuronal compensation by revealing a hypermetabolism (Bakhtiari et al., 2024; Benzinger et al., 2013; Oh et al., 2016) and later cognitive decline and thus neurodegeneration and hypometabolism (Förster et al., 2012; Landau et al., 2011). However, as approximately only half of the brain is composed of neurons while glia cells compose the other half (Bear et al., 2016a), it is reasonable that the [^{18}F]FDG PET signal is rather a combination of neuronal and glial glucose consumption, thus not reflecting solely the neuronal metabolism but also being influenced by e.g. inflammatory processes (Bartos et al., 2024; Carter et al., 2019; Gnörich et al., 2023; Ruch et al., 2024; Xiang et al., 2021). Thus, while [^{18}F]FDG is a widely used radiotracer, other tracers might give a more specific view on certain pathological processes by binding to targets that are directly involved in the desired read-out rather than assessing the secondary metabolic disturbances associated with pathological changes (Zhang et al., 2025).

3.2.2 [^{18}F]UCB-H

Given the rather unspecific information on neuronal integrity provided by [^{18}F]FDG, SV2A, being located in presynaptic vesicles and abundantly expressed in all areas of the brain, is an ideal candidate for assessing the synaptic density (Bajjalieh et al., 1994; Mendoza-Torreblanca et al., 2013). Consequently, several compounds deriving from the anti-epileptic drug levetiracetam were developed that bind with nanomolar affinity to SV2A (Mercier et al., 2014). Chen et al. (2018) then showed the effectiveness of a novel radiotracer, namely [^{11}C]-UCB-J, in a first in-human study. The tracer binds to SV2A which allows to show the density of presynaptic vesicles, however, the half-life of the radioisotope makes a use in clinical and preclinical practice challenging (Serrano et al., 2019). To overcome this problem, [^{18}F]UCB-H was developed (Warnier et al., 2016) and

there is increasing evidence that this fluorine-labelled radiotracer can be used as a reliable marker for synaptic density (Bastin et al., 2020; Bretin et al., 2013; Serrano et al., 2019; Vogler et al., 2023; Warnock et al., 2014). The first in-human-studies are already published, showing a significant uptake of [^{18}F]UCB-H in the brain (Bretin et al., 2015) and a correlation of [^{18}F]UCB-H uptake in the hippocampus with cognitive decline as measured by the Mini-Mental State Examination (MMSE) (Bastin et al., 2020).

3.2.3 [^{18}F]FBB

One major characteristic to distinguish AD from other forms of dementia is the pathological aggregation of Aβ fragments into plaques as mentioned in section 2.1.1. Several compounds are available to target amyloidosis and a PET scan with these radiotracers is now even strongly recommended to be included in the diagnosis of AD (Jack Jr. et al., 2024; Rabinovici et al., 2025; Zhang et al., 2025). Amongst those, [^{18}F]florbetaben ([^{18}F]FBB) has proven to be suitable in sensitivity and specificity for preclinical (Blume et al., 2018; Brendel et al., 2016; Rominger et al., 2013; Sacher et al., 2019, 2020; Waldron et al., 2015) as well as clinical PET imaging (Brendel et al., 2017; Dubois et al., 2023; Rowe et al., 2008).

3.2.4 [^{18}F]GE-180

The 18 kDa transclocator protein (TSPO) is expressed in microglia cells, mainly, but not exclusively, in the outer mitochondrial membrane. Under physiological conditions, TSPO is expressed in low levels, while they are rising when microglia become activated (Scarf et al., 2009; Scarf & Kassiou, 2011). [^{18}F]flutriciclamide ([^{18}F]GE-180) is a radiotracer specifically binding to TSPO (Fan et al., 2016; Liu et al., 2015; Zhang et al., 2025). The [^{18}F]GE-180 PET signal was shown to be rising throughout the ageing process as well as being increased in mouse models and human studies of neurodegenerative disorders (Blume et al., 2018; Brendel et al., 2016; Eckenweber et al., 2020; Kunze et al., 2023; Liu et al., 2015; Sacher et al., 2019, 2020; Xia et al., 2022), while also having potential for other diseases that are accompanied by an inflammation (Bartos et al., 2022; Zhang et al., 2025).

3.2.5 [^{18}F]F-DED

Monoamine oxidase B (MAO-B) showed to be a suitable target for the monitoring of reactive astrogliosis with PET. It is mainly expressed in the outer mitochondrial membrane of astrocytes and its expression is upregulated in the early phases of AD, when astrocytes become reactive due to protein accumulation and microglial activation (Carter et al., 2019; Ekblom et al., 1993; Olsen et al., 2017; Schedin-Weiss et al., 2017). [^{18}F]fluorodeprenyl-D_2 ([^{18}F]F-DED) showed a high affinity and specificity to MAO-B and has a reasonable half-life to be routinely used in preclinical and clinical imaging especially of neurodegenerative disorders (Ballweg et al., 2023; Nag et al., 2016).

3.3 Immunohistochemistry

Immunohistochemistry provides the possibility to obtain information about the abundance and location of selected proteins within a tissue. Therefore, the tissue needs to be treated with a fixation agent and, for most microscopes, cut in thin slices, although light sheet microscopy for whole organs is possible as well. Further, the selected proteins are labelled with a suitable primary and

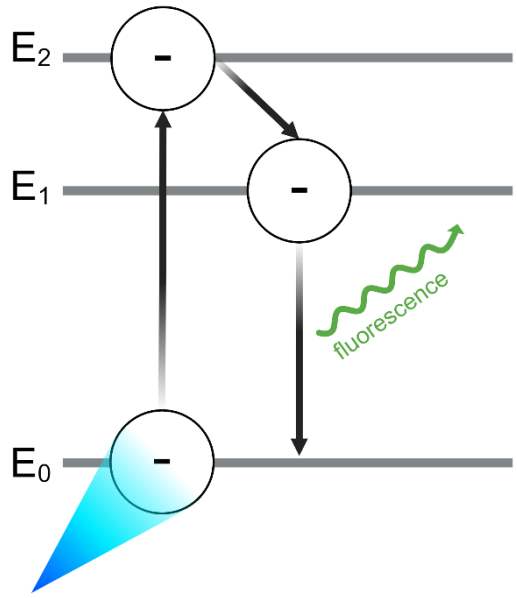

Figure 5 Simplified visualization of the principle of fluorescence with the excitation of an electron by an external source and subsequent change of the energetic state (E_2). While the electron falls back to its ground state (E_0) passing through an intermediate energy state (E_1), light of a lower wavelength compared to the excitation light is emitted. Based on Jabłoński (1933), Lichtman & Conchello (2005).

secondary antibody, of which the latter is attached to a fluorophore. The fluorophore can be excited by a certain wavelength lifting an electron to a higher energy state (E_2) followed by an emission of a lower-energy wavelength when the electron falls back to and intermediate state (E_1) and subsequently its ground state (E_0) (**Figure 5**). The emitted light can then be measured by a camera and the resulting image can be digitally optimized and processed (Alberts et al., 2022c; Buchwalow et al., 2023; Lichtman & Conchello, 2005).

For visualization of nucleic acid expression throughout the tissue, deoxyribonucleic acid (DNA) or ribonucleic acid (RNA) probes can be labelled with a fluorescent molecule attached to a complementary nucleic acid probe in a process called *in situ* hybridization. Fluorescence microscopy can then determine the expression of the specific ribonucleic acid probe within the tissue (Alberts et al., 2022c).

3.4 Behavioral Tests

Behavioral tests provide the possibility to examine the cognitive function of an animal in the context of normal ageing, disease models, and drug trials. Especially in AD research, the cognitive function is a major read-out for the degree of neurodegeneration and the subsequent memory loss especially in brain areas concerned with memory formation with the advantage of being decoupled from the yet unknown underlying pathological pathways (Bryan et al., 2009; Puzzo et al., 2014). Possibly unwanted variance in the results from behavioral testing can for example result from housing and previous handling of the animals, the overall excitation state of the animals, the time the behavioral test is performed within the animal's circadian rhythm, and the procedure of the behavioral test including the set-up and the handling of the equipment between different animals (Gould et al., 2009; Puzzo et al., 2014).

The open field test is a relatively easy behavioral test. The animal is placed into an arena and either observed or recorded in its behavior in response to the novel environment. Leaving the animal undisturbed during the test period, the open field provides a read-out of the normal activity considering the animal was given enough time to adopt to the novel environment. Thus, it is believed to provide information about the general behavior, including the emotional status of the animals. However, the set-up is prone to variation, making a comparison of open field tests in different laboratories difficult (Bryan et al., 2009; Gould et al., 2009).

The Morris Water Maze is a common test used to determine the long-term memory function of the mice. For this test, the animal is placed in a pool and is required to escape the water by climbing onto a platform, making use of the rodents' natural aversion to swimming. During several training rounds, the animal learns to find the platform using visual cues for orientation. On the test, the pool is filled with opaque water and the platform is removed. Read-outs indicating the memory performance of the animal tested include for example the amount of time needed to

reach the area where the platform was previously located, as well as the time spent in that area (Bear et al., 2016b; Bryan et al., 2009; Morris, 1981; Puzzo et al., 2014).

Other attempts to measure impairments in mice include the implementation of a frailty index as it was done for humans (Romero-Ortuno et al., 2010). Therefore, Whitehead et al. (2014) proposed a 31-point examination to assess age-related deficits in C57Bl/6 mice, revealing significant differences between age groups as well as a correlation with the human frailty index.

3.5 Biochemistry

Different types of cells can be distinguished by flow cytometry or fluorescent-activated cell sorting (FACS), where cells in a single-cell suspension are labelled with a fluorescent dye attached to a specific feature. Subsequently, based on their label, their number can be directly quantified and also separated into different populations for further analyses (Gompf, 2016).

Proteins can be quantified with different techniques. One possibility is Western blotting, where the proteins are separated based on their size using a gel matrix and electrical current, performing a sodium dodecyl sulfate polyacrylamide-gel electrophoresis (SDS-PAGE). Then, the proteins separated by SDS-PAGE are transferred to a membrane and are labelled with an antibody attached to a marker like a dye. The sensitivity can be as low as detecting less than 1 ng of protein (Alberts et al., 2022b). A second possibility for protein quantification are immunology-based techniques, where an antibody is binding to a specific antigen and the thus resulting complex is then labelled with an enzyme, allowing for a subsequent quantification based on the measured intensity using a standard curve as reference (Key, 2023; Rissin et al., 2010). Such techniques include the enzyme-linked immunosorbent assay (ELISA), as well as more sensitive techniques like electrochemiluminescence (ECL), where the detection involves applied voltage resulting in a measurable emission of light (Richter, 2004), or the single-molecule array (SiMoA), where a more than 100-fold higher sensitivity is achieved by establishing small chambers, thus reducing the volume where the reactions take place, coupled to a digital signal detection (Kuhle et al., 2016; Rissin et al., 2010).

Another possibility to differentiate macromolecules is column chromatography, e.g. liquid chromatography (LC). In this method, the solution containing the proteins or lipids to be detected is passed through one or several gel matrices within a column. The molecules separated by LC can further be identified by mass spectrometry (MS), unraveling the unique feature of their components' mass-to-charge ratio. Thus, these components can be identified and thereby the protein or lipid they were deriving from (Alberts et al., 2022b).

Quantitative analysis of RNA is most accurately done with the quantitative reverse transcription-polymerase chain reaction (RT-qPCR). RT-qPCR first performs a reverse transcription of the RNA to DNA, with the latter being subsequently amplified throughout multiple rounds of the polymerase chain reaction (PCR). With the attachment of fluorescent dyes, the concentration of the original RNA can be determined. Using RNA Sequencing (RNASeq), the relative expression levels of multiple RNAs can be determined, giving clues about up- or downregulated genes e.g. in response to a pathology or treatment (Alberts et al., 2022b).

4. Results and Discussion

In the first publication, we investigated the SV2A expression levels in the APPSL70 mouse model as well as its connection to Aβ plaque deposition and markers of neuroinflammation. While the APPSL70 mice do not show pronounced neurodegeneration during our observational period from five to eleven months of age, they expressed a profound fibrillary amyloidosis combined with cortical microglial activation, while astrocytic activation was present in subcortical regions, namely the thalamus, of eleven months old APPSL70 mice. This pathology is generally in line with previous studies on this mouse model (Blume et al., 2018).

In the second publication, we characterized a novel amyloidosis mouse model, introducing the Swedish, Arctic, and Austrian mutation to the mouse *App* gene. The model showed several key features of AD, including Aβ plaque deposition, neurodegeneration, neuroinflammation, a disturbed lipid metabolism, and behavioral changes (**Figure 6**). While other models achieve a plaque deposition by an overexpression of APP, we ensured that the full-length APP expression remained unaltered but rather the ratios of Aβ fragments changed. Thus, there was an early (two months of age) reduction in Aβ1-40 levels in the plasma. At four months of age, Aβ plaques steadily started to build up in the brain as measured with fluorescence imaging. The Aβ deposition further spread to the vasculature at eight months of age, leading to a cerebral amyloid angiopathy. In addition to amyloid, the APP^{SAA} mouse model displays a tauopathy, as the total tau levels were increased compared to the controls at eight months of age. Furthermore, dystrophic neurites could be found with immunohistochemical stainings in the brain of the APP^{SAA} mice at the same age. In accordance with the disturbance of the neuronal network, CSF NfL levels increased in this mouse model starting from two months of age and this increase became significant at 18 and 23 months of age. Neuroinflammation in response to protein accumulation presented itself with an increased microglia density around the plaques, as well as increased levels of TREM2 and different cytokines, accompanied by profound changes in the lipid metabolism. An increase in microglial activation could also be seen in TSPO-PET results, where APP^{SAA} mice had a significantly higher signal at twelve and 20 months of age compared to controls. Moreover, APP^{SAA} mice had changes in astrocytes with an upregulation of GFAP and downregulation of glutamate transporter 1 (GLT-1). Furthermore, APP^{SAA} mice displayed a significant hypermetabolism as measured by [^{18}F]FDG PET at twelve and 20 months of age that was associated with the [^{18}F]GE-180 PET signal. Behaviorally, the APP^{SAA} mice presented a hyperactivity phenotype and showed habituation deficits and an unusual preference for the center of the open field.

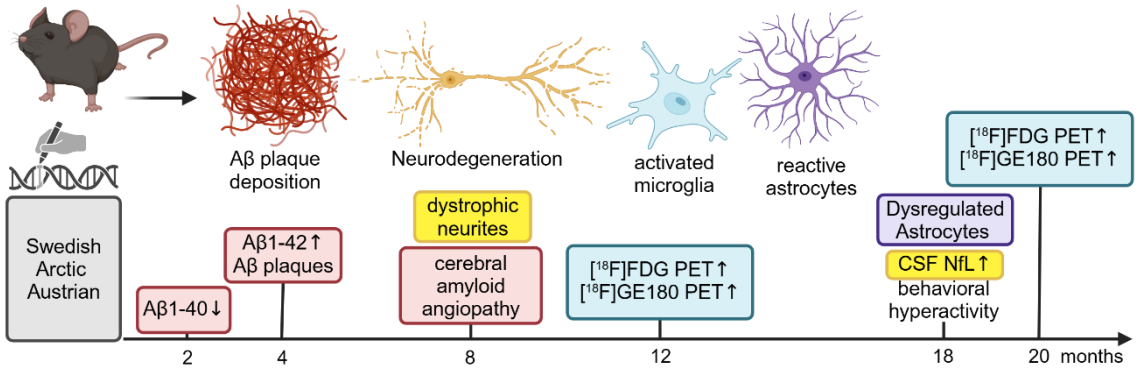

Figure 6 Pathological features of the APP^{SAA} mouse model harboring the Swedish, Arctic, and Austrian mutation in the *App* gene and their timely occurrence. Features of amyloidosis are marked in red features of neurodegeneration are marked in yellow, and features of neuroinflammation are marked in blue (microglial activation) and purple (astrocytic reactivity).

Thus, the APP^{SAA} mouse model shows several AD-related pathological changes, like Aβ aggregation, neurodegeneration, and neuroinflammation. Especially the disturbances in the microglia in the surrounding of Aβ plaques makes the APP^{SAA} mouse model a suitable tool to study the immune response and the mode of action of immunomodulatory agents in AD.

4.1 Aβ Deposition

Due to the respective genetic mutations, both the APPSL70 as well as the APP^{SAA} present with a widespread amyloidosis that was confirmed in previous and subsequent studies (Blume et al., 2018; Kim et al., 2025; Lu et al., 2025).

4.2 Neurodegeneration

The APP^{SAA} model showed signs of neurodegeneration in biomarker measurements, which manifested itself in a changing behavioral phenotype. In fact, a later study reported cognitive and motoric deficits as measured in several behavioral tests that occurred at 16 months of age (Blackmer-Raynolds et al., 2025).

A longitudinal assessment of pathological processes like neurodegeneration can be achieved with PET imaging. [^{18}F]FDG is a gold-standard measurement of neuronal integrity, although it actually provides only indirect read-out by measuring the cerebral metabolism (Ferris et al., 1980; Sokoloff et al., 1977). AD patients in an advanced stage show a significant hypometabolism (Bateman et al., 2012; Benzinger et al., 2013; Förster et al., 2012; Iaccarino et al., 2024; Landau et al., 2011) fitting the commonly known gradual neurodegenerative processes in AD patients (Bastin et al., 2020; Chen et al., 2018; Mecca et al., 2020; Terry et al., 1991). In contrast, AD mouse models showed a hypermetabolism (Ruch et al., 2024; Xia et al., 2022; Xiang et al., 2021), just as early AD patients (Bakhtiari et al., 2024; Benzinger et al., 2013). This increased cerebral metabolism was ascribed to activated immune cells, particularly microglia (Xiang et al., 2021). Based on these previous studies, this assumption was also made for the second publication, as the [^{18}F]GE-180 and [^{18}F]FDG PET signals showed a significant correlation.

In the first publication, we decided on a more direct read-out of neuronal integrity by choosing [^{18}F]UCB-H as PET tracer targeting SV2A. We saw a significant reduction in SV2A expression levels in the hippocampus and thalamus of both, APPSL70 and C57Bl/6 controls, from five to eleven months of age. Most likely, this reduction is due to the ageing of the mice (Cizeron et al., 2020). Rather surprisingly, we found a significant increase in the SV2A expression levels of APPSL70 mice compared to their C57Bl/6 counterparts in the [^{18}F]UCB-H PET signal as well as in the immunohistochemical analysis.

Bearing in mind that the APPSL70 mice do not show signs of neurodegeneration in the observed age, they are a model of the early phase of the disease with only amyloid pathology present. While SV2 was also found in dystrophic neurites, the SV2 abundancy was still lower in AD patients compared to cognitively normal controls (Snow et al., 1996). Thus, we suggest that the increase in SV2A expression in the APPSL70 mouse model is a compensatory mechanism shortly before neurodegeneration is measurable. In line with this hypothesis, Bell et al. (2003, 2007) found an upregulation of glutamatergic and GABAergic neurons before the onset of neurodegeneration in the TgCRND8 mouse model (Bell et al., 2003) as well as an increased density of glutamatergic

synapses in MCI patients (Bell et al., 2007). They also suggest the increase to be of a compensatory nature in response to hampered neuronal signaling by Aβ (Bell et al., 2007), which fits to the observed close similarity in group differences of APPSL70 and C57Bl/6 mice at eleven months of age in [^{18}F]UCB-H and [^{18}F]FBB PET signal. Moreover, an upregulation of synaptic activity or density in response to Aβ plaque deposition might exert negative effects by leading to hyperexcitability of neurons in AD, which was also found to be strongly associated with Aβ plaques (Busche et al., 2008; Targa Dias Anastacio et al., 2022). Thus, we see strong support for our hypothesis of a compensatory upregulation of synaptic activity or density in response to Aβ accumulation, ultimately further accelerating the process of neurodegeneration.

Neuronal hyperactivity is also reported for the APP^{SAA} model (Kim et al., 2025). However, Kim et al. (2025) described hyperemia and hyperactivity in the hippocampus before the onset of Aβ deposition in the APP^{SAA} mouse model, thus suggesting that unusually prolonged hyperemia adds to Aβ plaque deposition rather than being caused by the protein accumulation. Yet, this finding is in contrast to the correlation between the occurrence of Aβ plaques and hyperactive neurons that was described previously (Busche et al., 2008). Possibly, these two processes are mutually dependent. The exact mechanisms remain to be elucidated, however. Likewise, the first publication is limited by the lack of a mechanistic enquiry. To proof our hypothesis of a compensatory upregulation of SV2A in response to progressing amyloidosis, leading to hyperexcitability of the neuronal network, Ca^{2+}-imaging or electrophysiology would need to be applied on the APPSL70 mice.

4.3 Neuroinflammation

As reported previously for amyloidosis mouse models, Aβ plaque deposition was closely connected with microglial activation for both, the APPSL70 as well as the APP^{SAA} mouse model (Blume et al., 2018; Brendel et al., 2016; Sacher et al., 2020), which might further increase the hyperactivity in the neuronal network by the release of proinflammatory cytokines (Busche et al., 2008). Indeed, in the APP^{SAA} mouse model, activated microglia in close proximity to Aβ plaques displayed a major dysregulation of their metabolism. For the APPSL70 mice, SV2A expression levels, fibrillary amyloidosis, and microglial activation showed a high spatio-temporal agreement as assessed by SPM analysis. The calculation of the Dice-coefficient revealed a similarity of 53 % between respective group differences as calculated with SPM of SV2A and Aβ PET, and a similarity of 58 % between SPM images of SV2A and TSPO PET. An involvement of inflammatory cells would be interesting to further investigate by either depleting microglia at different time points or modulating their secreted factors.

In contrast, astrocytic reactivity as measured with [^{18}F]F-DED PET showed less similarity to the markers of SV2A expression, fibrillary amyloidosis, and microglial activity in the APPSL70 mouse model, as shown by a dice coefficient of only 26 % calculated for the spatio-temporal distribution patterns of SV2A and MAO-B PET. While we saw a significant increase in MAO-B expression levels in the thalamus at eleven months of age in the APPSL70 mice, previous studies described a widespread astrocytosis and a close connection of reactive astrocytes with Aβ plaques in different amyloidosis mouse models (Ballweg et al., 2023; Olsen et al., 2017). Possibly, this difference arises from the rather early time point (five to eleven months of age) we were investigating compared to up to 19 months of age (Ballweg et al., 2023) or up to 16 months of age (Olsen et al., 2017). Therefore, the astrocytosis might spread in later stages from the subcortical regions to a more cortical expression. Likewise, in the 18-months old APP^{SAA} mice, when signs of neurodegeneration were already present, a widespread astrocytic activation could be observed.

4.4 Concluding Remarks

In general, both studies show the high suitability of mouse models to study AD pathobiology at different stages. However, the simplicity of model organisms is often subject to critique, on the one hand as these models are only capable of displaying a part of the pathology (e.g. amyloidosis mouse models or models of tauopathy), and on the other hand as AD is a disease of ageing, thus naturally combining AD with different co-pathologies that are not present in an animal model (Rabinovici et al., 2025; Tai et al., 2021). Still, these limitations of model organisms also provide us with the opportunity to investigate selected mechanisms as well as distinguish between primary causes and secondary effects of AD (Tai et al., 2021), making mouse models an important tool to unravel the underlying mechanisms of neurodegenerative diseases. In that regard, AD models are of particular importance as it is a widespread disease among the elderly population, yet our understanding about the underlying pathobiology is limited. In addition, it is current consensus that the treatment of AD needs to focus on prevention of the disease before neuronal death and the development of suitable animal models is crucial for achieving this goal, as long as no comparable complex models are available to replace animal experiments (Sasaguri et al., 2017). Thus, the APP^{SAA} mouse model can provide novel insights, making use of a knock-in mechanism rather than an APP overexpression, avoiding potential artefacts introduced by a sheer surplus of APP protein levels (Sasaguri et al., 2017).

Longitudinal PET imaging of protein accumulation, neuroinflammation, and synaptic density provides the opportunity to evaluate the time course and connection of specific pathobiological processes, enabling the analysis of changing biomarkers within the same animal at different time points, thus reducing the number of animals needed for the study and aligning with the 3R principle of animal welfare (Cherry & Gambhir, 2001; Palumbo et al., 2023). In accordance with animal welfare, recommendations for imaging of small animals in cancer research include not more than three hours of imaging within 24 h and a maximum of five imaging sessions within one to two weeks (Workman et al., 2010). The mentioned guideline values align with our experience of what mice of different strains and with different pathologies (neurodegenerative and oncologic alike) generally tolerate.

Furthermore, PET imaging provides the unique opportunity to measure animal models and human patients with the same modality, thus bearing a high translational value (Cherry & Gambhir, 2001). Moreover, the increasing variety of PET tracers provides the opportunity to directly measure the extent of pathological processes. This feasibility is shown by various longitudinal and multi-tracer preclinical studies evaluating changes in the PET signal in mouse models of neurodegenerative diseases (Ballweg et al., 2023; Blume et al., 2018; Bouter et al., 2021; Brendel et al., 2016; Endepols et al., 2022; Maeda et al., 2007; Sacher et al., 2019, 2020; Vogler et al., 2023). However, most studies are using two different radiotracers at two to three different time points. In contrast, performing longitudinal PET scans with four different tracers at three time points within the same animals is rather rare and a unique feature of the first publication.

The possibility to assess mouse models with different PET tracers, thus visualizing changes in different proteins and pathways, enables a deeper insight into complex disorders. For example, in terms of neurodegenerative diseases, changes in synaptic density are of particular interest. Traditionally, the synaptic loss in AD was measured with a pronounced hypometabolism as seen in [^{18}F]FDG PET (Bateman et al., 2012; Benzinger et al., 2013; Endepols et al., 2022; Förster et al., 2012; Iaccarino et al., 2024; Landau et al., 2011). Measured with [^{18}F]UCB-H, this preclinical data shows that AD mouse models are not only experiencing a gradual neuronal loss, but rather facing a more complex phenomenon with likely a compensatory increase in SV2A expression levels reacting to the protein accumulation. This finding in turn sheds light on previously reported

observations of hypermetabolism in amyloidosis mouse models including the APP^{SAA} mice (Ruch et al., 2024; Xia et al., 2022; Xiang et al., 2021), showing that this phenomenon is not solely inflammation but might also reveal a connection to the measured hyperexcitability of neurons in response to Aβ deposition (Busche et al., 2008).

Concluding, to further explore the pathological features of AD and to prevent the disease by appropriate treatment before the onset of irreversible neurodegeneration, the research on animal models like the APP^{SAA} with suitable techniques with high translational ability like PET imaging is a key element.

5. References

Acioglu, C., Li, L., & Elkabes, S. (2021). Contribution of astrocytes to neuropathology of neurodegenerative diseases. *Brain Research*, *1758*, 147291. https://doi.org/10.1016/j.brainres.2021.147291

Alberts, B., Heald, R., Johnson, A., Morgan, D., Raff, M., Roberts, K., Walter, P., Wilson, J. H., & Hunt, T. (2022a). Chapter 5: DNA Replication, Repair, and Recombination. In *Molecular biology of the cell* (Seventh edition, international student edition, pp. 253–320). W. W. Norton & Company.

Alberts, B., Heald, R., Johnson, A., Morgan, D., Raff, M., Roberts, K., Walter, P., Wilson, J. H., & Hunt, T. (2022b). Chapter 8: Analyzing Cells, Molecules, and Systems. In *Molecular biology of the cell* (Seventh edition, international student edition, pp. 475–562). W. W. Norton & Company.

Alberts, B., Heald, R., Johnson, A., Morgan, D., Raff, M., Roberts, K., Walter, P., Wilson, J. H., & Hunt, T. (2022c). Chapter 9: Visualizing Cells and Their Molecules. In *Molecular biology of the cell* (Seventh edition, international student edition, pp. 563–602). W. W. Norton & Company.

Alzheimer, A. (1911). Über eigenartige Krankheitsfälle des späteren Alters. *Zeitschrift Für Die Gesamte Neurologie Und Psychiatrie*, *4*(1), 356–385.

Alzheimer's Association. (2024). 2024 Alzheimer's Disease Facts and Figures. *Alzheimer's & Dementia*, *20*(5), 1–147.

Bailey, D. L., Humm, J. L., Todd-Pokropek, A., & van Aswegen, A. (Eds.). (2014). *Nuclear Medicine Physics: A Handbook for Teachers and Students*. IAEA.

Bajjalieh, S. M., Frantz, G. D., Weimann, J. M., McConnell, S. K., & Scheller, R. H. (1994). Differential Expression of Synaptic Vesicle Protein 2 (SV2) lsoforms. *The Journal of Neuroscience*, *14*(9), 5223–5235.

Bakhtiari, A., Benedek, K., Law, I., Fagerlund, B., Mortensen, E. L., Osler, M., Lauritzen, M., Larsson, H. B. W., & Vestergaard, M. B. (2024). Early cerebral amyloid-β accumulation and hypermetabolism are associated with subtle cognitive deficits before accelerated cerebral atrophy. *GeroScience*, *46*, 769–782. https://doi.org/10.1007/s11357-023-01031-w

Ballweg, A., Klaus, C., Vogler, L., Katzdobler, S., Wind, K., Zatcepin, A., Ziegler, S. I., Secgin, B., Eckenweber, F., Bohr, B., Bernhardt, A., Fietzek, U., Rauchmann, B.-S., Stoecklein, S., Quach, S., Beyer, L., Scheifele, M., Simmet, M., Joseph, E., … Brendel, M. (2023). [^{18}F]F-DED PET imaging of reactive astrogliosis in neurodegenerative diseases: preclinical proof of concept and first-in-human data. *Journal of Neuroinflammation*, *20*, 68. https://doi.org/10.1186/s12974-023-02749-2

Bartos, L. M., Kirchleitner, S. V., Blobner, J., Wind, K., Kunze, L. H., Holzgreve, A., Gold, L., Zatcepin, A., Kolabas, Z. I., Ulukaya, S., Weidner, L., Quach, S., Messerer, D., Bartenstein, P., Tonn, J. C., Riemenschneider, M. J., Ziegler, S., von Baumgarten, L., Albert, N. L., & Brendel, M. (2022). 18 kDa translocator protein positron emission tomography facilitates early and robust tumor detection in the immunocompetent SB28 glioblastoma mouse model. *Frontiers in Medicine*, *9*, 992993. https://doi.org/10.3389/fmed.2022.992993

Bartos, L. M., Kunte, S. T., Wagner, S., Beumers, P., Schaefer, R., Zatcepin, A., Li, Y., Griessl, M., Hoermann, L., Wind-Mark, K., Bartenstein, P., Tahirovic, S., Ziegler, S., Brendel, M., & Gnörich, J. (2024). Astroglial glucose uptake determines brain FDG-PET alterations and metabolic connectivity during healthy aging in mice. *NeuroImage*, *300*, 120860. https://doi.org/10.1016/j.neuroimage.2024.120860

Bastin, C., Bahri, M. A., Meyer, F., Manard, M., Delhaye, E., Plenevaux, A., Becker, G., Seret, A., Mella, C., Giacomelli, F., Degueldre, C., Balteau, E., Luxen, A., & Salmon, E. (2020). In vivo imaging of synaptic loss in Alzheimer's disease with [18F]UCB-H positron emission tomography. *European Journal of Nuclear Medicine and Molecular Imaging*, *47*, 390–402. https://doi.org/10.1007/s00259-019-04461-x

Bateman, R. J., Xiong, C., Benzinger, T. L. S., Fagan, A. M., Goate, A., Fox, N. C., Marcus, D. S., Cairns, N. J., Xie, X., Blazey, T. M., Holtzman, D. M., Santacruz, A., Buckles, V., Oliver, A., Moulder, K., Aisen, P. S., Ghetti, B., Klunk, W. E., McDade, E., … Morris, J. C. (2012). Clinical and Biomarker Changes in Dominantly Inherited Alzheimer's Disease. *The New England Journal of Medicine*, *367*(9), 795–804. https://doi.org/10.1056/NEJMoa1202753

Beach, T. G., Monsell, S. E., Phillips, L. E., & Kukull, W. (2012). Accuracy of the Clinical Diagnosis of Alzheimer Disease at National Institute on Aging Alzheimer Disease Centers, 2005-2010. *Journal of Neuropathology & Experimental Neurology*, *71*(4), 266–273. https://doi.org/10.1097/NEN.0b013e31824b211b

Bear, M. F., Connors, B. W., & Paradiso, M. A. (2016a). Chapter 2: Neurons and Glia. In *Neuroscience: Exploring the Brain* (4th edition, pp. 23–54). Wolters Kluwer.

Bear, M. F., Connors, B. W., & Paradiso, M. A. (2016b). Chapter 24: Memory Systems. In *Neuroscience: Exploring the Brain* (4th edition, pp. 823–864). Wolters Kluwer.

Bell, K. F. S., Bennett, D. A., & Cuello, A. C. (2007). Paradoxical Upregulation of Glutamatergic Presynaptic Boutons during Mild Cognitive Impairment. *The Journal of Neuroscience*, *27*(40), 10810–10817. https://doi.org/10.1523/JNEUROSCI.3269-07.2007

Bell, K. F. S., de Kort, G. J. L., Steggerda, S., Shigemoto, R., Ribeiro-da-Silva, A., & Cuello, A. C. (2003). Structural involvement of the glutamatergic presynaptic boutons in a transgenic mouse model expressing early onset amyloid pathology. *Neuroscience Letters*, *353*, 143–147. https://doi.org/10.1016/j.neulet.2003.09.027

Benzinger, T. L. S., Blazey, T., Jack Jr., C. R., Koeppe, R. A., Su, Y., Xiong, C., Raichle, M. E., Snyder, A. Z., Ances, B. M., Bateman, R. J., Cairns, N. J., Fagan, A. M., Goate, A., Marcus, D. S., Aisen, P. S., Christensen, J. J., Ercole, L., Hornbeck, R. C., Farrar, A. M., … Morris, J. C. (2013). Regional variability of imaging biomarkers in autosomal dominant Alzheimer's disease. *Proceedings of the National Academy of Sciences*, *110*(47), E4502–E4509. https://doi.org/10.1073/pnas.1317918110

Blackmer-Raynolds, L., Lipson, L. D., Fraccaroli, I., Krout, I. N., Chang, J., & Sampson, T. R. (2025). Longitudinal characterization reveals behavioral impairments in aged APP knock in mouse models. *Scientific Reports*, *15*, 4631. https://doi.org/10.1038/s41598-025-89051-8

Blume, T., Focke, C., Peters, F., Deussing, M., Albert, N. L., Lindner, S., Gildehaus, F.-J., von Ungern-Sternberg, B., Ozmen, L., Baumann, K., Bartenstein, P., Rominger, A., Herms, J., & Brendel, M. (2018). Microglial response to increasing amyloid load saturates with aging: a longitudinal dual tracer in vivo μPET-study. *Journal of Neuroinflammation*, *15*, 307. https://doi.org/10.1186/s12974-018-1347-6

Bolós, M., Llorens-Martín, M., Jurado-Arjona, J., Hernández, F., Rábano, A., & Avila, J. (2016). Direct Evidence of Internalization of Tau by Microglia *In Vitro* and *In Vivo*. *Journal of Alzheimer's Disease*, *50*, 77–87. https://doi.org/10.3233/JAD-150704

Bouter, C., Irwin, C., Franke, T. N., Beindorff, N., & Bouter, Y. (2021). Quantitative Brain Positron Emission Tomography in Female 5XFAD Alzheimer Mice: Pathological Features and Sex-Specific Alterations. *Frontiers in Medicine*, *8*, 745064. https://doi.org/10.3389/fmed.2021.745064

Brendel, M., Probst, F., Jaworska, A., Overhoff, F., Korzhova, V., Albert, N. L., Beck, R., Lindner, S., Gildehaus, F.-J., Baumann, K., Bartenstein, P., Kleinberger, G., Haass, C., Herms, J., & Rominger, A. (2016). Glial Activation and Glucose Metabolism in a Transgenic Amyloid Mouse Model: A Triple-Tracer PET Study. *The Journal of Nuclear Medicine*, *57*(6), 954–960. https://doi.org/10.2967/jnumed.115.167858

Brendel, M., Schnabel, J., Schönecker, S., Wagner, L., Brendel, E., Meyer-Wilmes, J., Unterrainer, M., Schildan, A., Patt, M., Prix, C., Ackl, N., Catak, C., Pogarell, O., Levin, J., Danek, A., Buerger, K., Bartenstein, P., Barthel, H., Sabri, O., & Rominger, A. (2017). Additive value of amyloid-PET in routine cases of clinical dementia work-up after FDG-PET. *European Journal of Nuclear Medicine and Molecular Imaging*, *44*, 2239–2248. https://doi.org/10.1007/s00259-017-3832-z

Bretin, F., Bahri, M. A., Bernard, C., Warnock, G., Aerts, J., Mestdagh, N., Buchanan, T., Otoul, C., Koestler, F., Mievis, F., Giacomelli, F., Degueldre, C., Hustinx, R., Luxen, A., Seret, A., Plenevaux, A., & Salmon, E. (2015). Biodistribution and Radiation Dosimetry for the Novel SV2A Radiotracer [^{18}F]UCB-H: First-in-Human Study. *Molecular Imaging and Biology*, *17*, 557–564. https://doi.org/10.1007/s11307-014-0820-6

Bretin, F., Warnock, G., Bahri, M. A., Aerts, J., Mestdagh, N., Buchanan, T., Valade, A., Mievis, F., Giacomelli, F., Lemaire, C., Luxen, A., Salmon, E., Seret, A., & Plenevaux, A. (2013). Preclinical radiation dosimetry for the novel SV2A radiotracer [^{18}F]UCB-H. *EJNMMI Research*, *3*, 35. https://doi.org/10.1186/2191-219X-3-35

Bryan, K. J., Lee, H., Perry, G., Smith, M. A., & Casadesus, G. (2009). Transgenic Mouse Models of Alzheimer's Disease: Behavioral Testing and Considerations. In J. J. Buccafusco (Ed.), *Methods of Behavior Analysis in Neuroscience* (2nd edition). CRC Press/Taylor & Francis. https://www.ncbi.nlm.nih.gov/books/NBK5231/

Buchwalow, I. B., Böcker, W., & Tiemann, M. (2023). Immunhistochemie für Forschung und diagnostische Pathologie. In A. M. Raem & P. Rauch (Eds.), *Immunoassays: ergänzende Methoden, Troubleshooting, regulatorische Anforderungen* (2nd ed., pp. 317–337). Springer Spektrum. https://doi.org/10.1007/978-3-662-62671-9

Budd Haeberlein, S., Aisen, P. S., Barkhof, F., Chalkias, S., Chen, T., Cohen, S., Dent, G., Hansson, O., Harrison, K., von Hehn, C., Iwatsubo, T., Mallinckrodt, C., Mummery, C. J., Muralidharan, K. K., Nestorov, I., Nisenbaum, L., Rajagovindan, R., Skordos, L., Tian, Y., … Sandrock, A. (2022). Two Randomized Phase 3 Studies of Aducanumab in Early Alzheimer's Disease. *The Journal of Prevention of Alzheimer's Disease*, *9*(2), 197–210. https://doi.org/10.14283/jpad.2022.30

Busche, M. A., Eichhoff, G., Adelsberger, H., Abramowski, D., Wiederhold, K.-H., Haass, C., Staufenbiel, M., Konnerth, A., & Garaschuk, O. (2008). Clusters of Hyperactive Neurons Near Amyloid Plaques in a Mouse Model of Alzheimer's Disease. *Science*, *321*(5896), 1686–1689. https://doi.org/10.1126/science.1162844

Carter, S. F., Herholz, K., Rosa-Neto, P., Pellerin, L., Nordberg, A., & Zimmer, E. R. (2019). Astrocyte Biomarkers in Alzheimer's Disease. *Trends in Molecular Medicine*, *25*(2), 77–95. https://doi.org/10.1016/j.molmed.2018.11.006

Chatterjee, P., Pedrini, S., Doecke, J. D., Thota, R., Villemagne, V. L., Doré, V., Singh, A. K., Wang, P., Rainey-Smith, S., Fowler, C., Taddei, K., Sohrabi, H. R., Molloy, M. P., Ames, D., Maruff, P., Rowe, C. C., Masters, C. L., Martins, R. N., & the AIBL Research Group. (2023). Plasma Aβ42/40 ratio, p-tau181, GFAP, and NfL across the Alzheimer's disease continuum: A cross-sectional and longitudinal study in the AIBL cohort. *Alzheimer's & Dementia*, *19*, 1117–1134. https://doi.org/10.1002/alz.12724

Chen, M.-K., Mecca, A. P., Naganawa, M., Finnema, S. J., Toyonaga, T., Lin, S., Najafzadeh, S., Ropchan, J., Lu, Y., McDonald, J. W., Michalak, H. R., Nabulsi, N. B., Arnsten, A. F. T., Huang, Y., Carson, R. E., & van Dyck, C. H. (2018). Assessing Synaptic Density in Alzheimer Disease With Synaptic Vesicle Glycoprotein 2A Positron Emission Tomographic Imaging. *JAMA Neurology*, *75*(10), 1215–1224. https://doi.org/10.1001/jamaneurol.2018.1836

Cherry, S. R., & Dahlbom, M. (2006). *PET: Physics, Instrumentation, and Scanners* (M. E. Phelps, Ed.). Springer.

Cherry, S. R., & Gambhir, S. S. (2001). Use of Positron Emission Tomography in Animal Research. *ILAR Journal*, *42*(3), 219–232. https://doi.org/10.1093/ilar.42.3.219

Cizeron, M., Qiu, Z., Koniaris, B., Gokhale, R., Komiyama, N. H., Fransén, E., & Grant, S. G. N. (2020). A brainwide atlas of synapses across the mouse life span. *Science*, *369*(6501), 270–275. https://doi.org/10.1126/science.aba3163

Cohen, A. D., Landau, S. M., Snitz, B. E., Klunk, W. E., Blennow, K., & Zetterberg, H. (2019). Fluid and PET biomarkers for amyloid pathology in Alzheimer's disease. *Molecular and Cellular Neuroscience*, *97*, 3–17. https://doi.org/10.1016/j.mcn.2018.12.004

Davies, C. A., Mann, D. M. A., Sumpter, P. Q., & Yates, P. O. (1987). A quantitative morphometric analysis of the neuronal and synaptic content of the frontal and temporal cortex in patients with Alzheimer's disease. *Journal of the Neurological Sciences*, *78*(2), 151–164. https://doi.org/10.1016/0022-510X(87)90057-8

Deussing, M., Blume, T., Vomacka, L., Mahler, C., Focke, C., Todica, A., Unterrainer, M., Albert, N. L., Lindner, S., von Ungern-Sternberg, B., Baumann, K., Zwergal, A., Bartenstein, P., Herms, J., Rominger, A., & Brendel, M. (2018). Coupling between physiological TSPO expression in brain and myocardium allows stabilization of late-phase cerebral [^{18}F]GE180 PET quantification. *NeuroImage*, *165*, 83–91. https://doi.org/10.1016/j.neuroimage.2017.10.006

Dubois, B., von Arnim, C. A. F., Burnie, N., Bozeat, S., & Cummings, J. (2023). Biomarkers in Alzheimer's disease: role in early and differential diagnosis and recognition of atypical variants. *Alzheimer's Research & Therapy*, *15*, 175. https://doi.org/10.1186/s13195-023-01314-6

Eckenweber, F., Medina-Luque, J., Blume, T., Sacher, C., Biechele, G., Wind, K., Deussing, M., Briel, N., Lindner, S., Boening, G., von Ungern-Sternberg, B., Unterrainer, M., Albert, N. L., Zwergal, A., Levin, J., Bartenstein, P., Cumming, P., Rominger, A., Höglinger, G. U., … Brendel, M. (2020). Longitudinal TSPO expression in tau transgenic P301S mice predicts increased tau accumulation and deteriorated spatial learning. *Journal of Neuroinflammation*, *17*, 208. https://doi.org/10.1186/s12974-020-01883-5

Eckman, C. B., Mehta, N. D., Crook, R., Perez-tur, J., Prihar, G., Pfeiffer, E., Graff-Radford, N., Hinder, P., Yager, D., Zenk, B., Refolo, L. M., Prada, C. M., Younkin, S. G., Hutton, M., & Hardy, J. (1997). A new pathogenic mutation in the APP gene (I716V) increases the relative proportion of Aβ42(43). *Human Molecular Genetics*, *6*(12), 2087–2089. https://doi.org/10.1093/hmg/6.12.2087

Ekblom, J., Jossan, S. S., Bergström, M., Oreland, L., Walum, E., & Aquilonius, S.-M. (1993). Monoamine Oxidase-B in Astrocytes. *Glia*, *8*, 122–132. https://doi.org/10.1002/glia.440080208

Endepols, H., Anglada-Huguet, M., Mandelkow, E., Schmidt, Y., Krapf, P., Zlatopolskiy, B. D., Neumaier, B., Mandelkow, E.-M., & Drzezga, A. (2022). Assessment of the In Vivo Relationship Between Cerebral Hypometabolism, Tau Deposition, TSPO Expression, and Synaptic Density in a Tauopathy Mouse Model: a Multi-tracer PET Study. *Molecular Neurobiology*, *59*, 3402–3413. https://doi.org/10.1007/s12035-022-02793-8

Eurostat. (2025). *Causes of death—deaths by country of residence and occurrence* (hlth_cd_aro) [Dataset]. https://doi.org/10.2908/HLTH_CD_ARO

Ewers, M., Biechele, G., Suárez-Calvet, M., Sacher, C., Blume, T., Morenas-Rodriguez, E., Deming, Y., Piccio, L., Cruchaga, C., Kleinberger, G., Shaw, L., Trojanowski, J. Q., Herms, J., Dichgans, M., the Alzheimer's Disease Neuroimaging Initiative (ADNI), Brendel, M., Haass, C., & Franzmeier, N. (2020). Higher CSF sTREM2 and microglia activation are associated with slower rates of beta-amyloid accumulation. *EMBO Molecular Medicine*, *12*(9), e12308. https://doi.org/10.15252/emmm.202012308

Fakhoury, M. (2018). Microglia and Astrocytes in Alzheimer's Disease: Implications for Therapy. *Current Neuropharmacology*, *16*(5), 508–518. https://doi.org/10.2174/1570159X15666170720095240

Fan, Z., Calsolaro, V., Atkinson, R. A., Femminella, G. D., Waldman, A., Buckley, C., Trigg, W., Brooks, D. J., Hinz, R., & Edison, P. (2016). Flutriciclamide (^{18}F-GE180) PET: First-in-Human PET Study of Novel Third-Generation In Vivo Marker of Human Translocator Protein. *The Journal of Nuclear Medicine*, *57*(11), 1753–1759. https://doi.org/10.2967/jnumed.115.169078

Ferris, S. H., De Leon, M. J., Wolf, A. P., Farkas, T., Christman, D. R., Reisberg, B., Fowler, J. S., MacGregor, R., Goldman, A., George, A. E., & Rampal, S. (1980). Positron Emission Tomography in the Study of Aging and Senile Dementia. *Neurobiology of Aging*, *1*(2), 127–131. https://doi.org/10.1016/0197-4580(80)90005-6

Förster, S., Grimmer, T., Miederer, I., Henriksen, G., Yousefi, B. H., Graner, P., Wester, H.-J., Förstl, H., Kurz, A., Dickerson, B. C., Bartenstein, P., & Drzezga, A. (2012). Regional Expansion of Hypometabolism in Alzheimer's Disease Follows Amyloid Deposition with Temporal Delay. *Biological Psychiatry*, *71*(9), 792–797. https://doi.org/10.1016/j.biopsych.2011.04.023

Förstl, H., Bickel, H., & Perneczky, R. (2020). Alzheimer-Demenz und andere degenerative Demenzen. In P. Berlit (Ed.), *Klinische Neurologie* (pp. 1415–1430). Springer. https://doi.org/10.1007/978-3-662-60676-6

Gnörich, J., Reifschneider, A., Wind, K., Zatcepin, A., Kunte, S. T., Beumers, P., Bartos, L. M., Wiedemann, T., Grosch, M., Xiang, X., Fard, M. K., Ruch, F., Werner, G., Koehler, M., Slemann, L., Hummel, S., Briel, N., Blume, T., Shi, Y., … Brendel, M. (2023). Depletion and activation of microglia impact metabolic connectivity of the mouse brain. *Journal of Neuroinflammation*, *20*, 47. https://doi.org/10.1186/s12974-023-02735-8

Goate, A., Chartier-Harlin, M.-C., Mullan, M., Brown, J., Crawford, F., Fidani, L., Giuffra, L., Haynes, A., Irving, N., James, L., Mant, R., Newton, P., Rooke, K., Roques, P., Talbot, C., Pericak-Vance, M., Roses, A., Williamson, R., Rossor, M., … Hardy, J. (1991). Segregation of a missense mutation in the amyloid precursor protein gene with familial Alzheimer's disease. *Nature*, *349*, 704–706. https://doi.org/10.1038/349704a0

Gompf, A. (2016). Grundlagen der Durchflusszytometrie. In U. Sack (Ed.), *Zelluläre Diagnostik und Therapie* (pp. 1–28). De Gruyter.

Gould, T. D., Dao, D. T., & Kovacsics, C. E. (2009). The Open Field Test. In T. D. Gould (Ed.), *Mood and Anxiety Related Phenotypes in Mice* (Vol. 42, pp. 1–20). Humana Press. https://doi.org/10.1007/978-1-60761-303-9_1

Gustavsson, A., Norton, N., Fast, T., Frölich, L., Georges, J., Holzapfel, D., Kirabali, T., Krolak-Salmon, P., Rossini, P. M., Ferretti, M. T., Lanman, L., Chadha, A. S., & van der Flier, W. M. (2023). Global estimates on the number of persons across the Alzheimer's disease continuum. *Alzheimer's & Dementia*, *19*(2), 658–670. https://doi.org/10.1002/alz.12694

Haapasalo, A., & Kovacs, D. M. (2011). The Many Substrates of Presenilin/γ-Secretase. *Journal of Alzheimer's Disease*, *25*(1), 3–28. https://doi.org/10.3233/JAD-2011-101065

Hardy, J. A., & Higgins, G. A. (1992). Alzheimer's Disease: The Amyloid Cascade Hypothesis. *Science*, *256*(5054), 184–185. https://doi.org/10.1126/science.1566067

Heneka, M. T., Sastre, M., Dumitrescu-Ozimek, L., Hanke, A., Dewachter, I., Kuiperi, C., O'Banion, K., Klockgether, T., Van Leuven, F., & Landreth, G. E. (2005). Acute treatment with the PPARγ agonist pioglitazone and ibuprofen reduces glial inflammation and Aβ1–42 levels in APPV717I transgenic mice. *Brain*, *128*(6), 1442–1453. https://doi.org/10.1093/brain/awh452

Hickman, S. E., Allison, E. K., & El Khoury, J. (2008). Microglial Dysfunction and Defective β-Amyloid Clearance Pathways in Aging Alzheimer's Disease Mice. *The Journal of Neuroscience*, *28*(33), 8354–8360. https://doi.org/10.1523/JNEUROSCI.0616-08.2008

Huang, Y., & Mahley, R. W. (2014). Apolipoprotein E: Structure and function in lipid metabolism, neurobiology, and Alzheimer's diseases. *Neurobiology of Disease*, *72*, 3–12. https://doi.org/10.1016/j.nbd.2014.08.025

Iaccarino, L., Llibre-Guerra, J. J., McDade, E., Edwards, L., Gordon, B., Benzinger, T., Hassenstab, J., Kramer, J. H., Li, Y., Miller, B. L., Miller, Z., Morris, J. C., Mundada, N., Perrin, R. J., Rosen, H. J., Soleimani-Meigooni, D., Strom, A., Tsoy, E., Wang, G., … Rabinovici, G. D. (2024). Molecular neuroimaging in dominantly inherited versus sporadic early-onset Alzheimer's disease. *Brain Communications*, *6*(3), fcae159. https://doi.org/10.1093/braincomms/fcae159

Jack Jr., C. R., Andrews, J. S., Beach, T. G., Buracchio, T., Dunn, B., Graf, A., Hansson, O., Ho, C., Jagust, W., McDade, E., Molinuevo, J. L., Okonkwo, O. C., Pani, L., Rafii, M. S., Scheltens, P., Siemers, E., Snyder, H. M., Sperling, R., Teunissen, C. E., & Carrillo, M. C. (2024). Revised criteria for diagnosis and staging of Alzheimer's disease: Alzheimer's Association Workgroup. *Alzheimer's & Dementia*, *20*(8), 1–27. https://doi.org/10.1002/alz.13859

Jansen, W. J., Janssen, O., Tijms, B. M., Vos, S. J. B., Ossenkoppele, R., Visser, P. J., & Amyloid Biomarker Study Group. (2022). Prevalence Estimates of Amyloid Abnormality Across the Alzheimer Disease Clinical Spectrum. *JAMA Neurology*, *79*(3), 228–243. https://doi.org/10.1001/jamaneurol.2021.5216

Key, G. (2023). ELISA/EIA/FIA. In A. M. Raem & P. Rauch (Eds.), *Immunoassays: ergänzende Methoden, Troubleshooting, regulatorische Anforderungen* (2nd ed., pp. 53–71). Springer Spektrum. https://doi.org/10.1007/978-3-662-62671-9

Khan, Q. ul A., & Graff-Radford, N. R. (2017). Chapter 11: Alzheimer's Disease. In A. Schapira, Z. Wszolek, T. M. Dawson, & N. Wood (Eds.), *Neurodegeneration* (pp. 102–114). Wiley Blackwell.

Kim, T. A., Cruz, G., Syty, M. D., Wang, F., Wang, X., Duan, A., Halterman, M., Xiong, Q., Palop, J. J., & Ge, S. (2025). Neural circuit mechanisms underlying aberrantly prolonged functional hyperemia in young Alzheimer's disease mice. *Molecular Psychiatry*, *30*(2), 367–378. https://doi.org/10.1038/s41380-024-02680-9

Kuhle, J., Barro, C., Andreasson, U., Derfuss, T., Lindberg, R., Sandelius, Å., Liman, V., Norgren, N., Blennow, K., & Zetterberg, H. (2016). Comparison of three analytical platforms for quantification of the neurofilament light chain in blood samples: ELISA, electrochemiluminescence immunoassay and Simoa. *Clinical Chemistry and Laboratory Medicine (CCLM)*, *54*(10), 1655–1661. https://doi.org/10.1515/cclm-2015-1195

Kumar-Singh, S., De Jonghe, C., Cruts, M., Kleinert, R., Wang, R., Mercken, M., De Strooper, B., Vanderstichele, H., Löfgren, A., Vanderhoeven, I., Backhovens, H., Vanmechelen, E., Kroisel, P. M., & Van Broeckhoven, C. (2000). Nonfibrillar diffuse amyloid deposition due to a γ_{42}-secretase site mutation points to an essential role for N-truncated $A\beta_{42}$ in Alzheimer's disease. *Human Molecular Genetics*, *9*(18), 2589–2598.

Kunze, L. H., Ruch, F., Biechele, G., Eckenweber, F., Wind-Mark, K., Dinkel, L., Feyen, P., Bartenstein, P., Ziegler, S., Paeger, L., Tahirovic, S., Herms, J., & Brendel, M. (2023). Long-Term Pioglitazone Treatment Has No Significant Impact on Microglial Activation and Tau Pathology in P301S Mice. *International Journal of Molecular Sciences*, *24*(12), 10106. https://doi.org/10.3390/ijms241210106

Landau, S. M., Harvey, D., Madison, C. M., Koeppe, R. A., Reiman, E. M., Foster, N. L., Weiner, M. W., & Jagust, W. J. (2011). Associations between cognitive, functional, and FDG-PET measures of decline in AD and MCI. *Neurobiology of Aging*, *32*(7), 1207–1218. https://doi.org/10.1016/j.neurobiolaging.2009.07.002

Lichtenthaler, S. F. (2017). Predicting, Preventing, and Treating Alzheimer's Disease: Current State and Future Challenges. In M. Gadebusch Bondio, F. Spöring, & J.-S. Gordon (Eds.), *Medical Ethics, Prediction, and Prognosis: Interdisciplinary Perspectives* (1st ed., pp. 148–155). Routledge/Taylor & Francis Group.

Lichtman, J. W., & Conchello, J.-A. (2005). Fluorescence microscopy. *Nature Methods*, *2*(12), 910–919. https://doi.org/10.1038/nmeth817

Liu, B., Le, K. X., Park, M.-A., Wang, S., Belanger, A. P., Dubey, S., Frost, J. L., Holton, P., Reiser, V., Jones, P. A., Trigg, W., Di Carli, M. F., & Lemere, C. A. (2015). *In Vivo* Detection of Age- and Disease-Related Increases in Neuroinflammation by ^{18}F-GE180 TSPO MicroPET Imaging in Wild-Type and Alzheimer's Transgenic Mice. *The Journal of Neuroscience*, *35*(47), 15716–15730. https://doi.org/10.1523/JNEUROSCI.0996-15.2015

Logan, J., Fowler, J. S., Volkow, N. D., Wolf, A. P., Dewey, S. L., Schlyer, D. J., MacGregor, R. R., Hitzemann, R., Bendriem, B., Gatley, S. J., & Christman, D. R. (1990). Graphical Analysis of Reversible Radioligand Binding from Time-Activity Measurements Applied to [*N*-^{11}C-Methyl]-(−)-Cocaine PET Studies in Human Subjects. *Journal of Cerebral Blood Flow & Metabolism*, *10*(5), 740–747. https://doi.org/10.1038/jcbfm.1990.127

Lu, W., Shue, F., Kurti, A., Jeevaratnam, S., Macyczko, J. R., Roy, B., Izhar, T., Wang, N., Bu, G., Kanekiyo, T., & Li, Y. (2025). Amyloid pathology and cognitive impairment in hAβ-KI and APP^{SAA}-KI mouse models of Alzheimer's disease. *Neurobiology of Aging*, *145*, 13–23. https://doi.org/10.1016/j.neurobiolaging.2024.10.005

Maeda, J., Ji, B., Irie, T., Tomiyama, T., Maruyama, M., Okauchi, T., Staufenbiel, M., Iwata, N., Ono, M., Saido, T. C., Suzuki, K., Mori, H., Higuchi, M., & Suhara, T. (2007). Longitudinal, Quantitative Assessment of Amyloid, Neuroinflammation, and Anti-Amyloid Treatment in a Living Mouse Model of Alzheimer's Disease Enabled by Positron Emission Tomography. *Journal of Neuroscience*, *27*(41), 10957–10968. https://doi.org/10.1523/JNEUROSCI.0673-07.2007

Mao, R., Hu, M., Liu, X., Ye, L., Xu, B., Sun, M., Xu, S., Shao, W., Tan, Y., Xu, Y., Bai, F., & Shu, S. (2024). Impairments of GABAergic transmission in hippocampus mediate increased susceptibility of epilepsy in the early stage of Alzheimer's disease. *Cell Communication and Signaling*, *22*, 147. https://doi.org/10.1186/s12964-024-01528-7

MATLAB (Version 9.0.0.341360 (R2016a)). (2016). [Computer software]. The MathWorks Inc. https://www.mathworks.com

Mecca, A. P., Chen, M.-K., O'Dell, R. S., Naganawa, M., Toyonaga, T., Godek, T. A., Harris, J. E., Bartlett, H. H., Zhao, W., Nabulsi, N. B., Vander Wyk, B. C., Varma, P., Arnsten, A. F. T., Huang, Y., Carson, R. E., & van Dyck, C. H. (2020). In vivo measurement of widespread synaptic loss in Alzheimer's disease with SV2A PET. *Alzheimer's & Dementia*, *16*(7), 974–982. https://doi.org/10.1002/alz.12097

Mendoza-Torreblanca, J. G., Vanoye-Carlo, A., Phillips-Farfán, B. V., Carmona-Aparicio, L., & Gómez-Lira, G. (2013). Synaptic vesicle protein 2A: basic facts and role in synaptic function. *European Journal of Neuroscience*, *38*(11), 3529–3539. https://doi.org/10.1111/ejn.12360

Mercier, J., Archen, L., Bollu, V., Carré, S., Evrard, Y., Jnoff, E., Kenda, B., Lallemand, B., Michel, P., Montel, F., Moureau, F., Price, N., Quesnel, Y., Sauvage, X., Valade, A., & Provins, L. (2014). Discovery of Heterocyclic Nonacetamide Synaptic Vesicle Protein 2A (SV2A) Ligands with Single-Digit Nanomolar Potency: Opening Avenues towards the First SV2A Positron Emission Tomography (PET) Ligands. *ChemMedChem*, *9*(4), 693–698. https://doi.org/10.1002/cmdc.201300482

Mix, M. (2018). Positronen-Emissions-Tomographie. In W. Schlegel, C. P. Karger, & O. Jäkel (Eds.), *Medizinische Physik: Grundlagen – Bildgebung – Therapie – Technik* (pp. 349–364). Springer Spektrum. https://doi.org/10.1007/978-3-662-54801-1

Morris, R. G. M. (1981). Spatial Localization Does Not Require the Presence of Local Cues. *Learning and Motivation*, *12*(2), 239–260. https://doi.org/10.1016/0023-9690(81)90020-5

Mullan, M., Crawford, F., Axelman, K., Houlden, H., Lilius, L., Winblad, B., & Lannfelt, L. (1992). A pathogenic mutation for probable Alzheimer's disease in the APP gene at the N-terminus of β-amyloid. *Nature Genetics*, *1*, 345–347.

Nag, S., Fazio, P., Lehmann, L., Kettschau, G., Heinrich, T., Thiele, A., Svedberg, M., Amini, N., Leesch, S., Catafau, A. M., Hannestad, J., Varrone, A., & Halldin, C. (2016). In Vivo and In Vitro Characterization of a Novel MAO-B Inhibitor Radioligand, ^{18}F-Labeled Deuterated Fluorodeprenyl. *The Journal of Nuclear Medicine*, *57*(2), 315–320. https://doi.org/10.2967/jnumed.115.161083

Nasrolahi, A., Javaherforooshzadeh, F., Jafarzadeh-Gharehziaaddin, M., Mahmoudi, J., Dizaji Asl, K., & Shabani, Z. (2022). Therapeutic potential of neurotrophic factors in Alzheimer's Disease. *Molecular Biology Reports*, *49*, 2345–2357. https://doi.org/10.1007/s11033-021-06968-9

Nilsberth, C., Westlind-Danielsson, A., Eckman, C. B., Condron, M. M., Axelman, K., Forsell, C., Stenh, C., Luthman, J., Teplow, D. B., Younkin, S. G., Näslund, J., & Lannfelt, L. (2001). The 'Arctic' APP mutation (E693G) causes Alzheimer's disease by enhanced Aβ protofibril formation. *Nature Neuroscience*, *4*(9), 887–893. https://doi.org/10.1038/nn0901-887

Oh, H., Madison, C., Baker, S., Rabinovici, G., & Jagust, W. (2016). Dynamic relationships between age, amyloid-β deposition, and glucose metabolism link to the regional vulnerability to Alzheimer's disease. *Brain*, *139*(8), 2275–2289. https://doi.org/10.1093/brain/aww108

Olsen, M., Aguilar, X., Sehlin, D., Fang, X. T., Antoni, G., Erlandsson, A., & Syvänen, S. (2017). Astroglial Responses to Amyloid-Beta Progression in a Mouse Model of Alzheimer's Disease. *Molecular Imaging and Biology*, *20*, 605–614. https://doi.org/10.1007/s11307-017-1153-z

Palumbo, G., Kunze, L. H., Oos, R., Wind-Mark, K., Lindner, S., von Ungern-Sternberg, B., Bartenstein, P., Ziegler, S., & Brendel, M. (2023). Longitudinal Studies on Alzheimer Disease Mouse Models with Multiple Tracer PET/CT: Application of Reduction and Refinement Principles in Daily Practice to Safeguard Animal Welfare during Progressive Aging. *Animals*, *13*(11), 1812. https://doi.org/10.3390/ani13111812

Peretti, D. E., Boccalini, C., Ribaldi, F., Scheffler, M., Marizzoni, M., Ashton, N. J., Zetterberg, H., Blennow, K., Frisoni, G. B., & Garibotto, V. (2024). Association of glial fibrillary acid protein, Alzheimer's disease pathology and cognitive decline. *Brain*, *147*(12), 4094–4104. https://doi.org/10.1093/brain/awae211

Pike, V. W. (2009). PET Radiotracers: crossing the blood–brain barrier and surviving metabolism. *Trends in Pharmacological Sciences*, *30*(8), 431–440. https://doi.org/10.1016/j.tips.2009.05.005

Puzzo, D., Lee, L., Palmeri, A., Calabrese, G., & Arancio, O. (2014). Behavioral assays with mouse models of Alzheimer's disease: practical considerations and guidelines. *Biochemical Pharmacology*, *88*(4), 450–467. https://doi.org/10.1016/j.bcp.2014.01.011

Qi, J., & Leahy, R. M. (2006). Iterative reconstruction techniques in emission computed tomography. *Physics in Medicine and Biology*, *51*(15), R541–R578. https://doi.org/10.1088/0031-9155/51/15/R01

Qian, J., Wolters, F. J., Beiser, A., Haan, M., Ikram, M. A., Karlawish, J., Langbaum, J. B., Neuhaus, J. M., Reiman, E. M., Roberts, J. S., Seshadri, S., Tariot, P. N., McCarty Woods, B., Betensky, R. A., & Blacker, D. (2017). *APOE*-related risk of mild cognitive impairment and dementia for prevention trials: An analysis of four cohorts. *PLOS Medicine*, *14*(3), e1002254. https://doi.org/10.1371/journal.pmed.1002254

Rabinovici, G. D., Knopman, D. S., Arbizu, J., Benzinger, T. L. S., Donohoe, K. J., Hansson, O., Herscovitch, P., Kuo, P. H., Lingler, J. H., Minoshima, S., Murray, M. E., Price, J. C., Salloway, S. P., Weber, C. J., Carrillo, M. C., & Johnson, K. A. (2025). Updated appropriate use criteria for amyloid and tau PET: A report from the Alzheimer's Association and Society for Nuclear Medicine and Molecular Imaging Workgroup. *Alzheimer's & Dementia*, *21*(1), e14338. https://doi.org/10.1002/alz.14338

Ratni, H., Alker, A., Bartels, B., Bissantz, C., Chen, W., Gerlach, I., Limberg, A., Lu, M., Neidhart, W., Pichereau, S., Reutlinger, M., Rodriguez-Sarmiento, R.-M., Jakob-Roetne, R., Schmitt, G., Zhang, E., & Baumann, K. (2020). Discovery of RO7185876, a Highly Potent γ-Secretase Modulator (GSM) as a Potential Treatment for Alzheimer's Disease. *ACS Medicinal Chemistry Letters*, *11*(6), 1257–1268. https://doi.org/10.1021/acsmedchemlett.0c00109

Richter, M. M. (2004). Electrochemiluminescence (ECL). *Chemical Reviews*, *104*(6), 3003–3036. https://doi.org/10.1021/cr020373d

Rissin, D. M., Kan, C. W., Campbell, T. G., Howes, S. C., Fournier, D. R., Song, L., Piech, T., Patel, P. P., Chang, L., Rivnak, A. J., Ferrell, E. P., Randall, J. D., Provuncher, G. K., Walt, D. R., & Duffy, D. C. (2010). Single-molecule enzyme-linked immunosorbent assay detects serum proteins at subfemtomolar concentrations. *Nature Biotechnology*, *28*(6), 595–599. https://doi.org/10.1038/nbt.1641

Romero-Ortuno, R., Walsh, C. D., Lawlor, B. A., & Kenny, R. A. (2010). A Frailty Instrument for primary care: findings from the Survey of Health, Ageing and Retirement in Europe (SHARE). *BMC Geriatrics*, *10*, 57. https://doi.org/10.1186/1471-2318-10-57

Rominger, A., Brendel, M., Burgold, S., Keppler, K., Baumann, K., Xiong, G., Mille, E., Gildehaus, F.-J., Carlsen, J., Schlichtiger, J., Niedermoser, S., Wängler, B., Cumming, P., Steiner, H., Herms, J., Haass, C., & Bartenstein, P. (2013). Longitudinal Assessment of Cerebral β-Amyloid Deposition in Mice Overexpressing Swedish Mutant β-Amyloid Precursor Protein Using ^{18}F-Florbetaben PET. *The Journal of Nuclear Medicine*, *54*(7), 1127–1134. https://doi.org/10.2967/jnumed.112.114660

Rowe, C. C., Ackerman, U., Browne, W., Mulligan, R., Pike, K. L., O'Keefe, G., Tochon-Danguy, H., Chan, G., Berlangieri, S. U., Jones, G., Dickinson-Rowe, K. L., Kung, H. P., Zhang, W., Kung, M. P., Skovronsky, D., Dyrks, T., Holl, G., Krause, S., Friebe, M., … Villemagne, V. L. (2008). Imaging of amyloid β in Alzheimer's disease with ^{18}F-BAY94-9172, a novel PET tracer: proof of mechanism. *The Lancet Neurology*, *7*(2), 129–135. https://doi.org/10.1016/S1474-4422(08)70001-2

Ruch, F., Gnörich, J., Wind, K., Köhler, M., Zatcepin, A., Wiedemann, T., Gildehaus, F.-J., Lindner, S., Boening, G., von Ungern-Sternberg, B., Beyer, L., Herms, J., Bartenstein, P., Brendel, M., & Eckenweber, F. (2024). Validity and value of metabolic connectivity in mouse models of β-amyloid and tauopathy. *NeuroImage*, *286*, 120513. https://doi.org/10.1016/j.neuroimage.2024.120513

Sacher, C., Blume, T., Beyer, L., Biechele, G., Sauerbeck, J., Eckenweber, F., Deussing, M., Focke, C., Parhizkar, S., Lindner, S., Gildehaus, F.-J., von Ungern-Sternberg, B., Baumann, K., Tahirovic, S., Kleinberger, G., Willem, M., Haass, C., Bartenstein, P., Cumming, P., … Brendel, M. (2020). Asymmetry of Fibrillar Plaque Burden in Amyloid Mouse Models. *The Journal of Nuclear Medicine*, *61*(12), 1825–1831. https://doi.org/10.2967/jnumed.120.242750

Sacher, C., Blume, T., Beyer, L., Peters, F., Eckenweber, F., Sgobio, C., Deussing, M., Albert, N. L., Unterrainer, M., Lindner, S., Gildehaus, F.-J., von Ungern-Sternberg, B., Brzak, I., Neumann, U., Saito, T., Saido, T. C., Bartenstein, P., Rominger, A., Herms, J., & Brendel, M. (2019). Longitudinal PET Monitoring of Amyloidosis and Microglial Activation in a Second-Generation Amyloid-β Mouse Model. *The Journal of Nuclear Medicine*, *60*(12), 1787–1793. https://doi.org/10.2967/jnumed.119.227322

Sanchez-Crespo, A. (2013). Comparison of Gallium-68 and Fluorine-18 imaging characteristics in positron emission tomography. *Applied Radiation and Isotopes*, *76*, 55–62. https://doi.org/10.1016/j.apradiso.2012.06.034

Sánchez-Crespo, A., Andreo, P., & Larsson, S. A. (2004). Positron flight in human tissues and its influence on PET image spatial resolution. *European Journal of Nuclear Medicine and Molecular Imaging*, *31*(1), 44–51. https://doi.org/10.1007/s00259-003-1330-y

Sasaguri, H., Nilsson, P., Hashimoto, S., Nagata, K., Saito, T., De Strooper, B., Hardy, J., Vassar, R., Winblad, B., & Saido, T. C. (2017). APP mouse models for Alzheimer's disease preclinical studies. *The EMBO Journal*, *36*(17), 2473–2487. https://doi.org/10.15252/embj.201797397

Scarf, A. M., Ittner, L. M., & Kassiou, M. (2009). The Translocator Protein (18 kDa): Central Nervous System Disease and Drug Design. *Journal of Medicinal Chemistry*, *52*(3), 581–592. https://doi.org/10.1021/jm8011678

Scarf, A. M., & Kassiou, M. (2011). The Translocator Protein. *The Journal of Nuclear Medicine*, *52*(5), 677–680. https://doi.org/10.2967/jnumed.110.086629

Schedin-Weiss, S., Inoue, M., Hromadkova, L., Teranishi, Y., Yamamoto, N. G., Wiehager, B., Bogdanovic, N., Winblad, B., Sandebring-Matton, A., Frykman, S., & Tjernberg, L. O. (2017). Monoamine oxidase B is elevated in Alzheimer disease neurons, is associated with γ-secretase and regulates neuronal amyloid β-peptide levels. *Alzheimer's Research & Therapy*, *9*, 57. https://doi.org/10.1186/s13195-017-0279-1

Schindelin, J., Arganda-Carreras, I., Frise, E., Kaynig, V., Longair, M., Pietzsch, T., Preibisch, S., Rueden, C., Saalfeld, S., Schmid, B., Tinevez, J.-Y., White, D. J., Hartenstein, V., Eliceiri, K., Tomancak, P., & Cardona, A. (2012). Fiji: an open-source platform for biological-image analysis. *Nature Methods*, *9*(7), 676–682. https://doi.org/10.1038/nmeth.2019

Schlegel, W., Karger, C. P., & Jäkel, O. (Eds.). (2018). Teil III: Nuklearmedizinische Diagnostik und Therapie. In *Medizinische Physik: Grundlagen – Bildgebung – Therapie – Technik* (pp. 319–395). Springer Spektrum. https://doi.org/10.1007/978-3-662-54801-1

Sebastian Monasor, L., Müller, S. A., Colombo, A. V., Tanrioever, G., König, J., Roth, S., Liesz, A., Berghofer, A., Piechotta, A., Prestel, M., Saito, T., Saido, T. C., Herms, J., Willem, M., Haass, C., Lichtenthaler, S. F., & Tahirovic, S. (2020). Fibrillar Aβ triggers microglial proteome alterations and dysfunction in Alzheimer mouse models. *eLife*, *9*, e54083. https://doi.org/10.7554/eLife.54083

Serrano, M. E., Bahri, M. A., Becker, G., Seret, A., Mievis, F., Giacomelli, F., Lemaire, C., Salmon, E., Luxen, A., & Plenevaux, A. (2019). Quantification of [^{18}F]UCB-H Binding in the Rat Brain: From Kinetic Modelling to Standardised Uptake Value. *Molecular Imaging and Biology*, *21*, 888–897. https://doi.org/10.1007/s11307-018-1301-0

Snow, A. D., Nochlin, D., Sekiguchi, R., & Carlson, S. S. (1996). Identification and Immunolocalization of a New Class of Proteoglycan (Keratan Sulfate) to the Neuritic Plaques of Alzheimer's Disease. *Experimental Neurology*, *138*, 305–317. https://doi.org/10.1006/exnr.1996.0069

Sokoloff, L., Reivich, M., Kennedy, C., Des Rosiers, M. H., Patlak, C. S., Pettigrew, K. D., Sakurada, O., & Shinohara, M. (1977). THE [^{14}C]DEOXYGLUCOSE METHOD FOR THE MEASUREMENT OF LOCAL CEREBRAL GLUCOSE UTILIZATION: THEORY, PROCEDURE, AND NORMAL VALUES IN THE CONSCIOUS AND ANESTHETIZED ALBINO RAT. *Journal of Neurochemistry*, *28*(5), 897–916. https://doi.org/10.1111/j.1471-4159.1977.tb10649.x

Sperling, R. A., Aisen, P. S., Beckett, L. A., Bennett, D. A., Craft, S., Fagan, A. M., Iwatsubo, T., Jack Jr., C. R., Kaye, J., Montine, T. J., Park, D. C., Reiman, E. M., Rowe, C. C., Siemers, E., Stern, Y., Yaffe, K., Carrillo, M. C., Thies, B., Morrison-Bogorad, M., … Phelps, C. H. (2011). Toward defining the preclinical stages of Alzheimer's disease: Recommendations from the National Institute on Aging-Alzheimer's Association workgroups on diagnostic guidelines for Alzheimer's disease. *Alzheimer's & Dementia*, *7*(3), 280–292. https://doi.org/10.1016/j.jalz.2011.03.003

Statistical Parametric Mapping (Version 6685). (2016). [Computer software]. The Wellcome Trust Centre for Neuroimaging, Institute of Neurology, University College London. https://www.fil.ion.ucl.ac.uk/spm/software/spm12/

Statistisches Bundesamt (Destatis). (2024). *Zahl der Todesfälle wegen Alzheimer von 2003 bis 2023 fast verdoppelt*. https://www.destatis.de/DE/Presse/Pressemitteilungen/Zahl-der-Woche/2024/PD24_38_p002.html

Statistisches Bundesamt (Destatis). (2025). *Krankheitskosten, Krankheitskosten je Einwohner: Deutschland, Jahre, Krankheitsdiagnosen (ICD-10)* (23631–0001) [Dataset]. https://www-genesis.destatis.de/datenbank/online/statistic/23631/table/23631-0001/search/s/a3JhbmtoZWl0c2tvc3Rlbg==

Tai, L. M., Maldonado Weng, J., LaDu, M. J., & Brady, S. T. (2021). Chapter One—Relevance of transgenic mouse models for Alzheimer's disease. In D. B. Teplow (Ed.), *Molecular Biology of Neurodegenerative Diseases: Visions for the Future, Part B* (Vol. 177, pp. 1–48). Elsevier. https://doi.org/10.1016/bs.pmbts.2020.07.007

Targa Dias Anastacio, H., Matosin, N., & Ooi, L. (2022). Neuronal hyperexcitability in Alzheimer's disease: what are the drivers behind this aberrant phenotype? *Translational Psychiatry*, *12*, 257. https://doi.org/10.1038/s41398-022-02024-7

Terry, R. D., Masliah, E., Salmon, D. P., Butters, N., DeTeresa, R., Hill, R., Hansen, L. A., & Katzman, R. (1991). Physical Basis of Cognitive Alterations in Alzheimer's Disease: Synapse Loss Is the Major Correlate of Cognitive Impairment. *Annals of Neurology*, *30*(4), 572–580. https://doi.org/10.1002/ana.410300410

van der Weijden, C. W. J., Mossel, P., Bartels, A. L., Dierckx, R. A. J. O., Luurtsema, G., Lammertsma, A. A., Willemsen, A. T. M., & de Vries, E. F. J. (2023). Non-invasive kinetic modelling approaches for quantitative analysis of brain PET studies. *European Journal of Nuclear Medicine and Molecular Imaging*, *50*, 1636–1650. https://doi.org/10.1007/s00259-022-06057-4

van Dyck, C. H., Swanson, C. J., Aisen, P., Bateman, R. J., Chen, C., Gee, M., Kanekiyo, M., Li, D., Reyderman, L., Cohen, S., Froelich, L., Katayama, S., Sabbagh, M., Vellas, B., Watson, D., Dhadda, S., Irizarry, M., Kramer, L. D., & Iwatsubo, T. (2023). Lecanemab in Early Alzheimer's Disease. *The New England Journal of Medicine*, *388*(1), 9–21. https://doi.org/10.1056/NEJMoa2212948

Vogler, L., Ballweg, A., Bohr, B., Briel, N., Wind, K., Antons, M., Kunze, L. H., Gnörich, J., Lindner, S., Gildehaus, F.-J., Baumann, K., Bartenstein, P., Boening, G., Ziegler, S. I., Levin, J., Zwergal, A., Höglinger, G. U., Herms, J., & Brendel, M. (2023). Assessment of synaptic loss in mouse models of β-amyloid and tau pathology using [^{18}F]UCB-H PET imaging. *NeuroImage: Clinical*, *39*, 103484. https://doi.org/10.1016/j.nicl.2023.103484

Vossel, K. A., Beagle, A. J., Rabinovici, G. D., Shu, H., Lee, S. E., Naasan, G., Hegde, M., Cornes, S. B., Henry, M. L., Nelson, A. B., Seeley, W. W., Geschwind, M. D., Gorno-Tempini, M. L., Shih, T., Kirsch, H. E., Garcia, P. A., Miller, B. L., & Mucke, L. (2013). Seizures and Epileptiform Activity in the Early Stages of Alzheimer Disease. *JAMA Neurology*, *70*(9), 1158–1166. https://doi.org/10.1001/jamaneurol.2013.136

Voytyuk, I., De Strooper, B., & Chávez-Gutiérrez, L. (2018). Modulation of γ- and β-Secretases as Early Prevention Against Alzheimer's Disease. *Biological Psychiatry*, *83*(4), 320–327. https://doi.org/10.1016/j.biopsych.2017.08.001

Waldron, A.-M., Verhaeghe, J., Wyffels, L., Schmidt, M., Langlois, X., Van Der Linden, A., Stroobants, S., & Staelens, S. (2015). Preclinical Comparison of the Amyloid-β Radioligands [^{11}C]Pittsburgh compound B and [^{18}F]florbetaben in Aged APPPS1-21 and BRI1-42 Mouse Models of Cerebral Amyloidosis. *Molecular Imaging and Biology*, *17*, 688–696. https://doi.org/10.1007/s11307-015-0833-9

Warnier, C., Lemaire, C., Becker, G., Zaragoza, G., Giacomelli, F., Aerts, J., Otabashi, M., Bahri, M. A., Mercier, J., Plenevaux, A., & Luxen, A. (2016). Enabling Efficient Positron Emission Tomography (PET) Imaging of Synaptic Vesicle Glycoprotein 2A (SV2A) with a Robust and One-Step Radiosynthesis of a Highly Potent ^{18}F-Labeled Ligand ([^{18}F]UCB-H). *Journal of Medicinal Chemistry*, *59*(19), 8955–8966. https://doi.org/10.1021/acs.jmedchem.6b00905

Warnock, G. I., Aerts, J., Bahri, M. A., Bretin, F., Lemaire, C., Giacomelli, F., Mievis, F., Mestdagh, N., Buchanan, T., Valade, A., Mercier, J., Wood, M., Gillard, M., Seret, A., Luxen, A., Salmon, E., & Plenevaux, A. (2014). Evaluation of ^{18}F-UCB-H as a Novel PET Tracer for Synaptic Vesicle Protein 2A in the Brain. *The Journal of Nuclear Medicine*, *55*(8), 1336–1341. https://doi.org/10.2967/jnumed.113.136143

Whitehead, J. C., Hildebrand, B. A., Sun, M., Rockwood, M. R., Rose, R. A., Rockwood, K., & Howlett, S. E. (2014). A Clinical Frailty Index in Aging Mice: Comparisons With Frailty Index Data in Humans. *The Journals of Gerontology: Series A*, *69*(6), 621–632. https://doi.org/10.1093/gerona/glt136

Wolf, S. A., Boddeke, H. W. G. M., & Kettenmann, H. (2017). Microglia in Physiology and Disease. *Annual Review of Physiology*, *79*, 619–643. https://doi.org/10.1146/annurev-physiol-022516-034406

Wolfe, M. S. (2021). Probing Mechanisms and Therapeutic Potential of γ-Secretase in Alzheimer's Disease. *Molecules*, *26*(2), 388. https://doi.org/10.3390/molecules26020388

Workman, P., Aboagye, E. O., Balkwill, F., Balmain, A., Bruder, G., Chaplin, D. J., Double, J. A., Everitt, J., Farningham, D. A. H., Glennie, M. J., Kelland, L. R., Robinson, V., Stratford, I. J., Tozer, G. M., Watson, S., Wedge, S. R., Eccles, S. A., & An *ad hoc* committee of the National Cancer Research Institute. (2010). Guidelines for the welfare and use of animals in cancer research. *British Journal of Cancer*, *102*, 1555–1577. https://doi.org/10.1038/sj.bjc.6605642

Xia, D., Lianoglou, S., Sandmann, T., Calvert, M., Suh, J. H., Thomsen, E., Dugas, J., Pizzo, M. E., DeVos, S. L., Earr, T. K., Lin, C.-C., Davis, S., Ha, C., Leung, A. W.-S., Nguyen, H., Chau, R., Yulyaningsih, E., Lopez, I., Solanoy, H., … Sanchez, P. E. (2022). Novel *App* knock-in mouse model shows key features of amyloid pathology and reveals profound metabolic dysregulation of microglia. *Molecular Neurodegeneration*, *17*, 41. https://doi.org/10.1186/s13024-022-00547-7

Xiang, X., Wind, K., Wiedemann, T., Blume, T., Shi, Y., Briel, N., Beyer, L., Biechele, G., Eckenweber, F., Zatcepin, A., Lammich, S., Ribicic, S., Tahirovic, S., Willem, M., Deussing, M., Palleis, C., Rauchmann, B.-S., Gildehaus, F.-J., Lindner, S., … Brendel, M. (2021). Microglial activation states drive glucose uptake and FDG-PET alterations in neurodegenerative diseases. *Science Translational Medicine*, *13*(615), eabe5640. https://doi.org/10.1126/scitranslmed.abe5640

Yiannopoulou, K. G., & Papageorgiou, S. G. (2020). Current and Future Treatments in Alzheimer Disease: An Update. *Journal of Central Nervous System Disease*, *12*, 1–12. https://doi.org/10.1177/1179573520907397

Yokoyama, M., Kobayashi, H., Tatsumi, L., & Tomita, T. (2022). Mouse Models of Alzheimer's Disease. *Frontiers in Molecular Neuroscience*, *15*, 912995. https://doi.org/10.3389/fnmol.2022.912995

Zhang, S., Wang, X., Gao, X., Chen, X., Li, L., Li, G., Liu, C., Miao, Y., Wang, R., & Hu, K. (2025). Radiopharmaceuticals and their applications in medicine. *Signal Transduction and Targeted Therapy*, *10*, 1. https://doi.org/10.1038/s41392-024-02041-6

6. First Publication

Kunze, L. H., Palumbo, G., Gnörich, J., Wind-Mark, K., Schaefer, R., Lindner, S., Gildehaus, F.-J., Ziegler, S., & Brendel, M. (2025). Fibrillar amyloidosis and synaptic vesicle protein expression progress jointly in the cortex of a mouse model with β-amyloid pathology. *NeuroImage*, *310*, 121165. https://doi.org/10.1016/j.neuroimage.2025.121165

7. Second Publication

Xia, D., Lianoglou, S., Sandmann, T., Calvert, M., Suh, J. H., Thomsen, E., Dugas, J., Pizzo, M. E., DeVos, S. L., Earr, T. K., Lin, C.-C., Davis, S., Ha, C., Leung, A. W.-S., Nguyen, H., Chau, R., Yulyaningsih, E., Lopez, I., Solanoy, H., … , **Kunze, L. H.**, … , Sanchez, P. E. (2022). Novel *App* knock-in mouse model shows key features of amyloid pathology and reveals profound metabolic dysregulation of microglia. *Molecular Neurodegeneration*, *17*, 41. https://doi.org/10.1186/s13024-022-00547-7

Danksagung

Die vorliegende Arbeit wäre ohne die Unterstützung einiger Menschen nicht möglich gewesen.

Ganz besonders gilt mein Dank meiner Doktormutter, Prof. Dr. Sibylle Ziegler, die bereitwillig meine Betreuung übernommen hat und mich die gesamte Zeit sowohl fachlich als auch persönlich unterstützt hat. Liebe Frau Ziegler, vielen Dank für die Zeit, die Sie sich für jedes Gespräch genommen haben, für die Gespräche auf Augenhöhe und für Ihre wunderbare Betreuung. Ich habe sehr viel von Ihnen gelernt und hätte mir keine bessere Doktormutter wünschen können.

Bei Prof. Dr. Dr. Matthias Brendel möchte ich mich herzlich für das Vertrauen in meine Fähigkeiten und Entscheidungen bedanken. Ich erinnere mich gerne an unser erstes Gespräch, das mich direkt von der Nuklearmedizin und meinem ersten Projekt begeistert hat. Seit meinem Start in der „Nuk“ als wissenschaftliche Mitarbeiterin habe ich in unseren wöchentlichen Meetings viel gelernt. Lieber Matthias, vielen Dank, dass ich mit Dir über alle Ergebnisse offen diskutieren konnte und Du immer ein offenes Ohr für alle meine Ideen hattest. Du hast mir viele Möglichkeiten eröffnet und mir die Chance gegeben, ständig neue Erfahrungen zu sammeln und mich fachlich wie persönlich weiterzuentwickeln.

Die Erfahrungen als Doktorandin hängen immer stark von dem Umfeld ab, in dem man diese Zeit verbringt. Ich hatte das Glück, in das beste Team zu kommen, das man sich dafür vorstellen kann. Das große Projekt, mit dem ich gestartet bin, wäre nie erfolgreich gewesen ohne Giovanna Palumbo, die mich bei stundenlangen PET-Scans tatkräftig unterstützt hat und dabei mit Kaffee und Schokolade die Laune gehoben hat. Für die Hilfe bei den PET-Scans möchte ich mich auch bei Karin Wind-Mark bedanken, die mir gerade am Anfang zusätzlich mit ständiger tierärztlicher Beratung zur Seite gestanden hat und vor allem über mehrere Wochen Verhaltenstests an den Tieren durchgeführt hat. Giovanna und Karin, ich hätte mein Projekt mit niemandem lieber durchführen wollen. Vielen Dank für Eure Unterstützung und Eure Freundschaft! Mein Dank gilt außerdem Rosel Oos, die stets bereit war, bei PET-Scans mitzuhelfen und die erste Anlaufstelle für Fragen rund ums Labor war. Danken möchte ich auch dem gesamten Team der Präklinik, in dem jeder bereit ist, sich gegenseitig zu unterstützen.

Für die Synthese der Radiotracer möchte ich dem gesamten Team der Radiochemie danken und besonders Dr. Franz-Josef „Uffi“ Gildehaus, der mir [^{18}F]FBB wöchentlich meisterhaft zuverlässig in einer Handsynthese hergestellt hat und für den Erfolg der Projekte auch die ein oder andere Extrasynthese in Kauf genommen hat.

Herzlich danken möchte ich auch Dr. Astrid Delker und Prof. Dr. Guido Böning, die mich liebenswerterweise in das „Physik & Friends“ Team aufgenommen haben und mich sowohl fachlich wie auch persönlich immer gut beraten haben. Astrid, ich bin Dir besonders dankbar, dass Du mir direkt einen Platz in der Vorlesung angeboten hast und ich damit schon während der Doktorarbeit mit der Lehre starten konnte. Vielen Dank, dass Du stets ein offenes Ohr für mich hast und Deine Erfahrungen mit mir teilst.

Schließlich möchte ich dem gesamten Team der Nuklearmedizin unter der Leitung von Prof. Dr. Peter Bartenstein und, seit Beginn diesen Jahres, Prof. Dr. Rudolf Alexander Werner danken.

Während meiner Zeit in der „Nuk“ habe ich die beste Gruppe kennengelernt, die es gibt. Isabelle Fuxjäger, Marlies Härtel, Manvir Lalia, Sandra Resch und Rebecca Schäfer, wir haben zusammen einige Höhepunkte gefeiert und Tiefpunkte überstanden. Ich bin unendlich dankbar, immer Eure Unterstützung gehabt zu haben. Worte können nicht ausdrücken, wie wichtig mir Eure Freundschaft geworden ist.

Und zuletzt gilt mein Dank meiner Familie und besonders der wichtigsten Person in meinem Leben: Bene, Du musstest über die Jahre so einiges mitmachen und Dir alles zu PET-Bildgebung, Alzheimer und meinen Projekten im Speziellen anhören. Vielen Dank, dass Du stets mein geduldiger Berater warst, mich aufgebaut hast, wenn ich verzweifelt war, mich regelmäßig aus meiner Komfortzone geholt hast und Dich für jeden Erfolg mit mir gefreut hast. Ohne Deine Unterstützung hätte ich mich vermutlich weder getraut, nach meinem Bachelor of Arts einen naturwissenschaftlichen Master anzufangen, noch mich für eine Doktorarbeit zu bewerben, geschweige denn irgendetwas davon abzuschließen.